

Article

# A Mineralized Alga and Acritarch Dominated Microbiota from the Tully Formation (Givetian) of Pennsylvania, USA

John A. Chamberlain Jr. <sup>1,2,\*</sup>, Rebecca B. Chamberlain <sup>3</sup> and James O. Brown <sup>4</sup>

<sup>1</sup> Department of Earth and Environmental Sciences, Brooklyn College, Brooklyn, NY 11210, USA

<sup>2</sup> PhD Programs in Earth and Environmental Science and Biology, City University of New York, Graduate Center, New York, NY 10016, USA

<sup>3</sup> Department of Biology, College of Staten Island, Staten Island, NY 10314, USA; rebecca.chamberlain@csi.cuny.edu

<sup>4</sup> Department of Environmental Sciences, William Paterson University, Wayne, NJ 07470, USA; brownj1@wpunj.edu

\* Correspondence: johnc@brooklyn.cuny.edu; Tel.: +1-718-591-5416

Academic Editors: Olaf Lenz and Jesus Martinez-Frias

Received: 12 September 2016; Accepted: 13 December 2016; Published: 19 December 2016

**Abstract:** Sphaeromorphic algal cysts, most probably of the prasinophyte *Tasmanites*, and acanthomorphic acritarch vesicles, most probably *Solisphaeridium*, occur in a single 20 cm thick bed of micritic limestone in the lower part of the Middle Devonian (Givetian) Tully Formation near Lock Haven, Pennsylvania. Specimens are composed of authigenic calcite and pyrite crystals about 5–10 µm in length. Some specimens are completely calcitic; some contain both pyrite and calcite; and many are composed totally of pyrite. The microfossils are about 80 to 150 µm in diameter. Many show signs of originally containing a flexible wall composed of at least two layers. Some appear to have been enclosed in a mucilaginous sheath or membrane when alive. The acanthomorphic forms have spines that are up to 20 µm in length, expand toward the base, and are circular in cross-section. The microflora occurs with microscopic molluscs, dactyloconarids, the enigmatic *Jinonicella*, and the oldest zooecia of ctenostome bryozoans known from North America. The microalgal horizon lacks macrofossils although small burrows are present. Microalgae and acritarchs have been preserved via a complex preservational process involving rapid, bacterially-mediated post-mortem mineralization of dead cells. The microfossil horizon, and possibly much of the Tully Formation at Lock Haven with similar lithology, formed in a relatively deep, off-shore basin with reduced oxygen availability in the substrate.

**Keywords:** microalgae; acritarchs; *Jinonicella*; ctenostome zooecia; Tully Formation; Givetian; Pennsylvania

## 1. Introduction

The presence in Paleozoic rocks of mineralized, walled, microscopic spheroids has been known since the work of Williamson [1] on the paleobotany of the English coal measures. Williamson [1] described these microscopic structures as calcareous spheroidal bodies about 50 to 500 µm in diameter and enclosed by a dark, usually multi-layered wall. There are two main types: those that have a smooth outer surface, and those having a surface studded with numerous conical spines or cylindrical spikes. Williamson [1] referred to the smooth surfaced forms as calcispheres, a name by which they are sometimes still identified. The spiny, acanthomorphic forms have been referred to as radiosphaerids or radiosphaerid calcispheres [2]. Although some authors have questioned the organic status of calcispheres [3–5], there is little doubt now that they are indeed the remains of once living organisms.

There, has been much debate, however, as to what kind or kinds of organisms they are. They have been referred to as foraminifers [6,7]; radiolarians [1]; and algae [8,9].

Complicating this picture are microfossils known informally as mazuelloids [10,11], and formally named *Muellerisphaerida* by Kozur [12]. These objects are identical to some radiosphaerid calcispheres in terms of size and morphology, but are composed, not of carbonate as are radiosphaerids, but of microcrystalline phosphate. The identity of mazuelloids, and their connection to calcispheres has been a controversial issue. Mazuelloids have been considered as possible radiolarians [12], foraminifera [10], and dinoflagellates [13]. Adding to this complexity are isolated occurrences of pyritic microscopic, spheroidal objects of organic origin from Paleozoic rocks of Europe [14,15], as well as from the United States [16].

Considering the diversity of opinion on the identity of Paleozoic mineralized spheroidal microfossils, the most reasonable approach is to follow the proposal of Kaźmierczak et al. [17] who argue that calcispheres are a polyphyletic grouping of organic walled microorganisms that have been calcified post-mortally. Likewise, Kremer [18] presents a strong argument that mazuelloids are organic-walled microorganisms that have been preserved through a process of post-mortem phosphatization. Unless there is sufficient evidence to convincingly place material into a definite taxon, it is probably best to follow the suggestion of Kremer [18] and Kaźmierczak and Kremer [2] to temporarily view mineralized organic spheroids as members of the Acritarcha, an informal grouping of eukaryotic microorganisms of uncertain affinities [19–22]. However, the recent application of atomic force microscopy, confocal microscopy, Raman spectroscopy, and other sophisticated analytic techniques to the study of the ultrastructure, life history, and systematic affinities of mineralized, but originally organic-walled microfossils [23–27], has shown that some acritarchs are actually fossilized microalgae. In the end, it may well be, as Moczydłowska et al. [28] have suggested, that many acritarchs will, in fact, turn out to be algae. It should be noted, however, that idiosyncrasies of fossil acritarch and algal preservational processes can generate results that mimic other organisms or their components [29,30]. Advancement in this endeavor will thus probably be difficult.

In this paper we describe microscopic mineralized spheroidal bodies, which we interpret as microalgae and acritarchs, preserved in the Middle Devonian (Givetian) Tully Formation of north-central Pennsylvania. The Tully objects include both smooth surfaced, sphaeromorphic forms, and spiny, acanthomorphic forms. While some specimens are calcitic, many specimens are composed of pyrite, and some contain both minerals. We also describe other micro-organisms preserved with the microspheroids, including the enigmatic *Jinonicella* and the earliest known North American ctenostome bryozoan zoecia, and consider the identity, mode of formation, preservational history, and paleoecology of the Tully microfossils.

## 2. Materials and Methods

### 2.1. Geologic Setting

The Tully Formation is a prominent member of the Middle Devonian sequence in the Northern Appalachian Basin of Pennsylvania and New York (in this paper New York means New York State rather than New York City), and has been the focus of study for more than a century [31–39]. In Pennsylvania the Tully Formation is exposed in a long, sinuous outcrop belt (Figure 1A) produced by the combined effects of Late Paleozoic Appalachian tectonism and subsequent erosion. Our specimens come from Lock Haven, Pennsylvania, which lies in the central part of this exposure belt (Figure 1A). At Lock Haven, the Tully Formation is exposed on the north bank of the West Branch of the Susquehanna River immediately west of the north end of the Jay Street Bridge which crosses the river from the center of Lock Haven (Figure 1B). The original land surface has been steepened by excavation for Pennsylvania highway route 664, and it is in this roadcut that the Tully Formation is exposed.

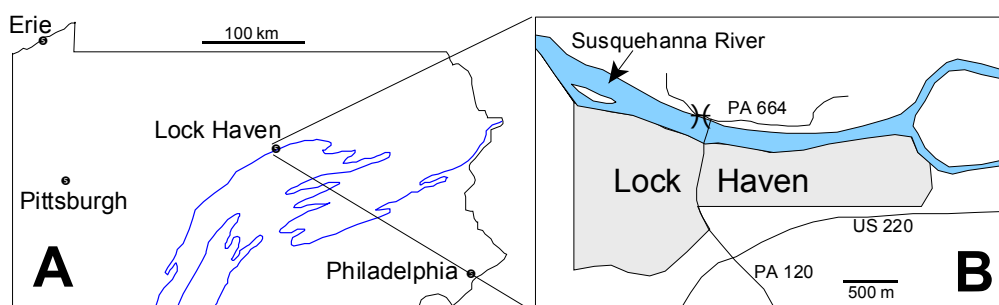


**Figure 1.** Locality Maps. (A) Map of Pennsylvania showing the location of Lock Haven. The main outcrop belt of the Tully Formation and its lateral equivalents is shown in the blue line; (B) Detailed map of the Lock Haven area. Star shows the site of the Tully exposure from which the microfossils described here derive. PA664 and PA120 refer to Pennsylvania state highways. US220 identifies a US federal highway. North is toward the top of the page in both maps.

In central and western New York, the Tully Formation is composed primarily of limestone and shaley limestone. The Tully Formation is notable as the only significant carbonate unit within the otherwise siliciclastic Middle Devonian rocks of the Appalachian Basin. However, to the east, the Tully Formation becomes increasingly siliciclastic and in the Catskill area of New York it interfingers with the terrestrial siltstones and shales of the Gilboa Formation [35]. Ammonoid and conodont zonations indicate that the age of the Tully Formation in New York is uppermost Givetian [38,40,41]. This interpretation is consistent with conodont data from the Burkett Member, the lowermost unit of the Harrell Shale, which directly overlies the Tully Formation in central and western Pennsylvania and is recognized as lowermost Frasnian [42].

In Pennsylvania, the Tully Formation usually occurs as a relatively thin (<10 m thick), dominantly carbonate unit divisible according to Heckel [36,37] by a prominent intraformational discontinuity into an upper and lower member. Above this discontinuity the upper member is usually abundantly fossiliferous with assemblages dominated by corals, brachiopods, trilobites, and molluscs (see Heckel [37] for Tully species lists). Below this discontinuity, Heckel's lower member is much less fossiliferous with respect to macrofossils. However, dacryoconarids, hollow, conical microfossils of uncertain affinities, are common and widespread [36]. More recently, Baird and Brett [38,39] have developed a detailed correlational model for the Tully Formation across its range in New York and Pennsylvania that is both utilitarian and well supported by field evidence. These authors recognize a three-fold division of the Tully Formation in which Heckel's lower unit is subdivided into two different depositional sequences separated by a discontinuity that Baird and Brett [38,39] interpret as a maximum flooding surface. Baird and Brett [38,39] point out that, in addition, a number of regional discontinuities occur in different parts of the Tully outcrop belt, so that the bed by bed content of Tully exposures, as well as the nature of its contacts with units above and below, varies considerably over the outcrop range of the formation.

At Lock Haven the Tully Formation has been studied most notably by Willard [33,34], Heckel [36,37], and Baird and Brett [38,39]. All agree that below the discontinuity flooring Heckel's upper Tully member, the unit is unusually thick (Figure 2). Baird and Brett [38] note that this thickening at Lock Haven is due primarily to increase in the thickness of their middle Tully Taughannock Falls beds relative to the thickness of these beds elsewhere. The occurrence at the eastern end of the Lock Haven outcrop of such index brachiopods as *Camarotoechia mesocostale*, *Rhysochonetes aurora*, and *Emanuella subumbona* indicate very clearly that at least part of Baird and Brett's [38] New Lisbon interval of their lower Tully depositional sequence is present at Lock Haven, as is at least part of the Windom Member of the Moscow Formation beneath the Tully. However, the partially to totally covered aspect of the Lock Haven exposure over this part of the sequence, has hindered deciphering of its stratigraphic details.

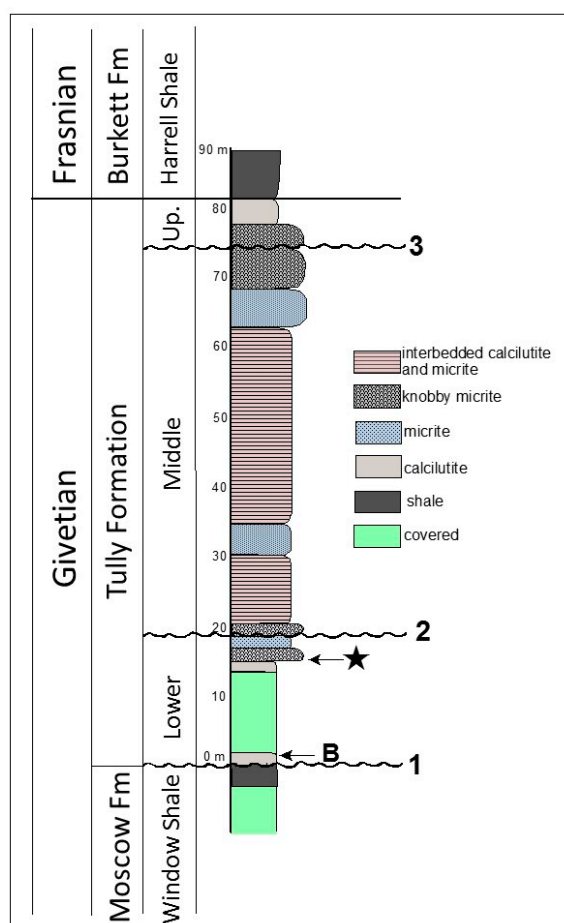


**Figure 2.** Stratigraphic column for the Lock Haven exposure of the Tully Formation. Star indicates the position of the microfossils described here. B indicates the position from which the index brachiopods *Camarotoechia mesocostale*, *Rhyssochonetes aurora*, and *Emanuella subumbona* were recovered. Discontinuities: 1—discontinuity at Tully/Moscow contact; 2—inferred position of discontinuity representing the maximum flooding surface of Baird and Brett [38,39] separating the Lower and Middle Tully Formation; 3—Heckel’s [36,37] disconformity defining the base of the Upper Tully Formation.

## 2.2. Microfossil Occurrence

The Lock Haven Tully Formation exposure consists predominately of two interbedded lithologies: (1) finely laminated calcilutite; and (2) calcilutite with a dense micritic texture. The latter beds are more resistant to weathering and form prominent ledges in the roadcut (Figure 3A). Many of the micritic calcilutites in the exposure have a distinct knobby appearance, and break apart into rounded, irregular fragments. The microalgae, acritarchs, and other microfossils we describe here derive from a single 20 cm thick horizon at the base of the lowermost ledge-forming, knobby calcilutite bed in the Tully exposure (Figures 2 and 3A,B). This bed lies approximately 14.6 m above the contact with the underlying Moscow Formation; 59.9 m below the discontinuity at the base of the Upper Tully Formation, and 64.9 m below the contact between the Upper Tully Formation and the overlying Burkett Member of the Harrell Shale, as measured by Brown [43], and confirmed by us in 2014. The stratigraphic position of the microalgal bed relative to underlying fine-grained, calcareous shale beds containing *Emanuella*, *Camarotoechia*, and *Rhyssochonetes* indicate that the microfossils derive from beds that are probably equivalent to lower Carpenters Falls beds of Baird and Brett [38], and thus are part of Baird and Brett’s [38,39] lower Tully depositional sequence. This places the microfossil horizon within the Taghanic faunal interval discussed by these authors. The microalgal bed and the fossils it contains were thus involved in the lower Tully Bioevent [38,39,44] which records the incursion of Old

World faunal elements into the Appalachian Basin and the concurrent disappearance of endemic North American forms. This episode is the early phase of the Global Frasnian Biocrisis which re-structured the biotic composition of the ocean both regionally in the Northern Appalachian Basin [38,39,44–46] and globally [47–50] via eradication of much of the provincialism that had characterized Lower Devonian faunas.

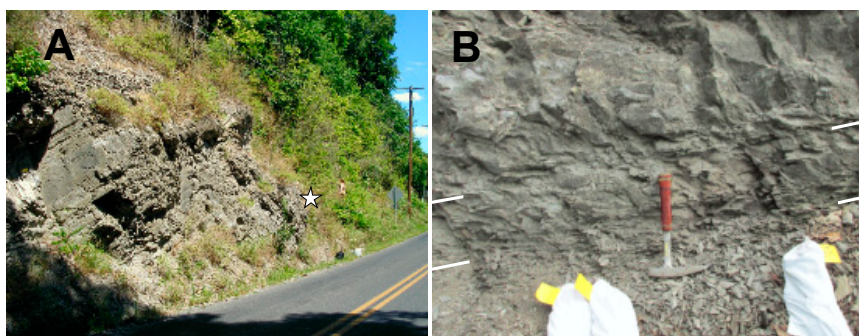


**Figure 3.** Microfossil outcrop, Lock Haven, PA. (A) Lower Tully Formation looking east along PA route 644. The lowermost knobby micritic calcilutites referred to in the text form the prominent ledge in the left foreground. Star shows the position of the microfossil horizon. Below these beds the exposure is heavily vegetated, but float indicates that the underlying rock is calcareous shale. The Tully-Windom contact lies past the utility pole at the right margin of the figure; (B) Close-up of the microfossil bed (between the white hachures) showing its irregular, knobby appearance. The top of the uppermost finely laminated, fissile calcareous shale typical of the beds extending down to the Tully-Windom contact can be seen below the microfossil bed. Hammer handle is about 25 cm long.

The microfossil bed (Figure 3B) is black to dark gray in color on fresh surfaces, but weathers to light gray. No macrofossils co-occur with the microfossils, although irregular, pyritized burrows up to 10 cm in length and 2 mm in diameter are not uncommon. Shorter burrows up to 1 cm in diameter also occur. All of our material comes from two rock samples, each weighing approximately two kilograms, taken from a single location in this bed so that the lateral extent of microfossil occurrence within this horizon is not known. We collected rock samples somewhat higher in this ledge also, from beds physically similar to the microfossil horizon but no pyritized specimens were found. It would appear from these observations that with the exception of dacryoconarids [36], microfossils may not be widely dispersed in rocks of the Lower Tully Formation at the Lock Haven site, but clearly a more sophisticated sampling regimen than the one used here will be needed to ascertain their distribution, both laterally and vertically.

### 2.3. Preparation Methods

One of our two kilogram rock samples was processed for microfossils using a procedure based on the microfossil preparation methods described by Harris and Sweet [51] and Maples and Waters [52]. The untreated sample was reduced in a rock crusher to chips 6 cm in diameter or less. This material was then softened and further reduced by a series of formic acid baths. To facilitate disaggregation, the material was heated and quenched in cold water between acid baths as described by Pojeta and Balanc [53]. Reduction was further enhanced by soaking in Stoddard's solvent and bleach prior to each re-application of formic acid. To concentrate the heavy (high density) material, the acid bath residue was passed through a sodium metatungstate (SMT) solution following the procedures of Krukowski [54] and Harris and Sweet [51]. SMT specific gravity was set between that of quartz and apatite. This allowed us to capture essentially all pyritic material in the residue. Several SMT filtrations were required to do this. Pyritic microfossils were removed manually from the heavy fraction using stereozoom binocular microscopes. We visually checked the lighter filtrate for phosphatic microfossils. None were found.

The preparation technique we used here differs considerably from the strong acid reduction procedures normally used to obtain organic-walled and phosphatized microfossils. It is, however, very similar to the preparation methods Loydell et al. [14] used in their discovery of pyritic mazuelloids in Sweden and Wales. This situation suggests to us that preparation methodology may have a strong influence on the recovery potential of pyritic microalgae and perhaps on other pyritic microfossils as well. Thus, the perceived rarity of pyritic, as compared to phosphatic, microfossil occurrences may reflect preparation technique. Pyritic microalgae and other microfossils may actually be more widely distributed than is currently recognized.

Another aspect of the preparation method we used is whether or not it has distorted our perception of the Tully microbiota by systematically excluding certain groups of organisms from detection. While this is clearly a possibility, we doubt that such exclusions are extensive. We see no compelling reason to believe that other palynomorphs, particularly those that were originally composed of organic compounds (e.g., scolecodonts, chitinozoans, spores, cyanobacteria), would not be subject to the same mineralization processes that operated on the organic walled organisms that we do find in the Tully microbiota. It is our opinion that such absence reflects life habits or habitat preferences that are inconsistent with the severely dysoxic Tully depositional environment as discussed below. Further work using different preparation procedures would be helpful in resolving this issue, but this lies outside the scope of the present work.

#### 2.4. SEM Methods

Some pyritized specimens illustrated in this paper were plated with 40 nm of gold and imaged in a JEOL-6301 scanning electron microscope located in the Physics Department, Brooklyn College. Most specimens were plated with a platinum/gold mix and imaged using an Amray digital SEM located in the College of Staten Island Advanced Imaging Facility (AIF). Elemental analysis was done on selected pyritized specimens using an AIF Amray EDX analyzer.

#### 2.5. Thin Section Methods

We thin-sectioned material taken from our second outcrop sample of the microfossil bed as well as from micrite beds up to 3 m stratigraphically higher. These samples were sectioned both parallel and vertical to bedding. Thin section analysis was used as means of determining the original, pre-extraction abundance and state of microfossils in the limestone. Thirty-seven thin sections were examined in this study.

#### 2.6. Specimen Repository

All thin sections and SEM-imaged specimens discussed here have been deposited in the paleontological collections of the Department of Earth and Environmental Sciences, Brooklyn College, Brooklyn, NY, USA. Thin sections carry the ID prefix, TYT; SEM specimens have the ID prefix, TYS.

### 3. Results

#### 3.1. Thin Section Results

##### 3.1.1. Rock Texture

The texture of the lowermost knobby calcilutite beds and the character of microfossil distribution within this horizon are illustrated in the micrographs shown in Figure 4. Figure 4A shows the dense, microcrystalline micrite composing these calcilutite beds. The slightly darker central region of the figure is actually a burrow cross-section, while the lighter, slightly more macrocrystalline region outside the burrow is the micrite itself. Minute dark grains of pyrite can be seen thinly disseminated throughout the micrograph, particularly within the burrow. However, large, pyritized masses within the burrow indicative of fecal material are absent. Figure 4B shows another burrow containing abundant small

pyrite grains. The surrounding micrite in Figure 4B also contains pyrite, but not nearly as abundantly as the burrow. Again fecal material is not obvious. Schieber [55] interpreted similar occurrences of disseminated burrow pyrite in the Ordovician Black Island Member of the Winnipeg Formation in Saskatchewan as developing from organic substrates contained in slime trails and mucus produced by burrow makers and other benthic organisms. He noted that such occurrences are bacterially mediated and are indicative of a rapid mineralization process.

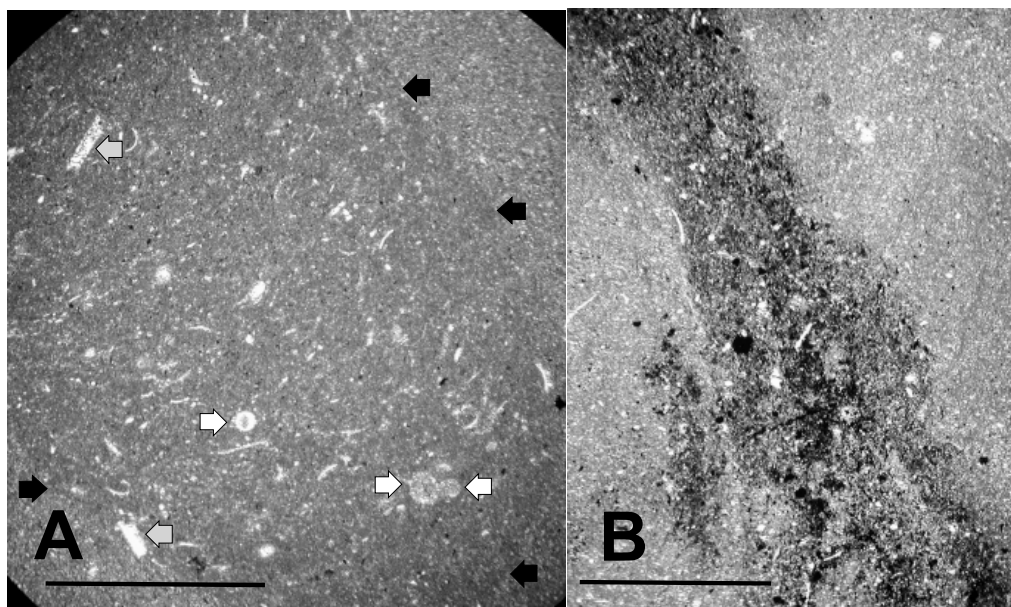


**Figure 4.** Texture of the Lower Tully Formation microfossil bed. (A) thin section (TYT-11) cut parallel to bedding showing burrow cross-section. The burrow appears as the slightly darker, more microcrystalline region in the center of the picture (periphery highlighted by black arrows). Small black masses of pyrite can be seen widely disseminated within the burrow. Also inside the burrow are a small number of circular objects (white arrows), and numerous sparry structures, some of which are shell fragments (gray arrows). Scale bar = 1 mm; (B) thin section (TYT-23) cut perpendicular to bedding showing a pyrite-rich burrow. Scale bar = 750  $\mu\text{m}$ .

As suggested in Figure 4, pyrite in the form of small grains is a common constituent of the microfossil bed, and often is concentrated in the burrows that occur within this horizon. We do not see evidence in thin section that pyrite occurs in discrete laminations or occurs in stratiform layers, although the knobby structure of the calcilutite seen in outcrop suggests a stromatolitic structuring for at least some of the calcilutite beds. We did not explicitly test for this, however, so that further work is needed to resolve this point.

### 3.1.2. Shell Fragments

Crystalline objects other than pyrite grains are also visible in Figure 3. These are mainly of two forms. Among the most common are small, tabular and curved objects, which are composed of highly birefringent, sparry calcite crystals larger than the micrite crystals of the groundmass. Two of the larger examples are highlighted in Figure 4A with gray arrows. Like the pyrite grains, these objects are more common within the burrows than outside them. We interpret these structures as fragments of mollusc shell or dacroconarid test, in which the original carbonate microarchitecture has been secondarily recrystallized to form the sparry grains seen here. In the case of mollusc shell fragments, the size of the whole shells from which the pieces derive is indicated from their curvature as being probably no larger than about 1–2 mm.

### 3.1.3. Microalga and Acritarch Remains

In addition to bits of shell, the rock contains small spheroidal objects, such as those identified by white arrows in Figure 4A. These objects we interpret as microalgal and acritarch vesicles. They are at least as abundant as shell fragments, and are commonly seen in the thin sections we have examined. As intimated in Figure 4, they vary somewhat in the details of their microarchitecture, and in size. Some have diameters between about 70  $\mu\text{m}$ , and 150  $\mu\text{m}$ , as in Figure 4, but many are larger.

One of these microfossils is shown in greater detail in Figure 5A. It is circular in cross section and has a diameter of about 150  $\mu\text{m}$ . Its interior is filled with sparry calcite crystals up to about 10 times the size of the micrite grains surrounding the specimen. A halo of elongate sparry calcite crystals oriented with their long axes perpendicular to the specimen adheres to its outer surface. This halo is similar to rings of prismatic calcite grains surrounding calcitic acritarchs (calcspheres) preserved in Late Devonian limestones of Poland [2] (Figures 1–9), [26] (Figure 2). A similar ring of such prismatic crystals, but smaller in size, adheres to the inner surface of the Tully specimen shown in Figure 5. Such inner halos are not as common as the outer ones. Figure 5B, C show that where the specimen's outer wall is not obliterated by formation of these crystalline halos the wall is defined by three distinct dark-colored bands, each with a thickness of about 1  $\mu\text{m}$ . Between these dark bands are two light colored bands about 3  $\mu\text{m}$  in thickness. Thus, the total thickness of the wall is about 8–10  $\mu\text{m}$ . Although simple, unlayered vesicle walls are typical of the prasinophyte alga *Tasmanites*, the multi-layered wall seen in Figure 5 is suggestive of the wall structure encountered in some species of this genus, e.g., *Tasmanites sommeri* Winslow [56]. However, *T. sommeri* has more wall laminations, (10–12 according to Winslow [56]), and with much smaller inter-laminar spacing than is apparent in the specimen illustrated in Figure 5. The trilaminar sheath structure, common in the vesicle walls of leiosphaerid microalgae [28], is not seen in the specimen illustrated in Figure 5.

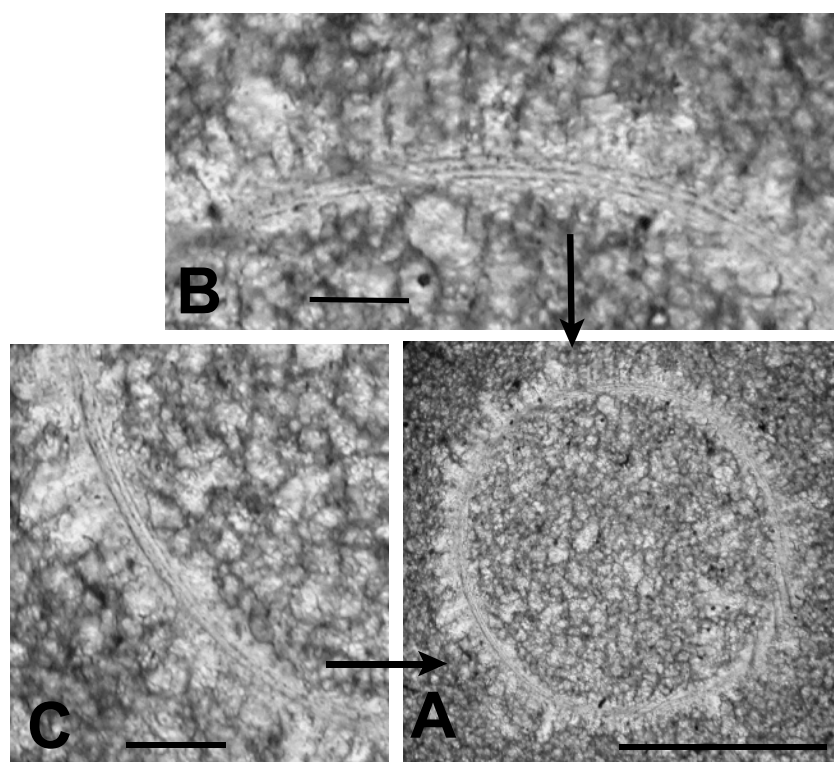


**Figure 5.** Microalgal cell (TYT-05) viewed in white light. (A) specimen in cross-section surrounded by micrite. Scale bar = 100  $\mu\text{m}$ ; (B) enlargement of the upper portion of specimen showing a multi-layered body wall defined by three thin, dark bands. Scale bar = 20  $\mu\text{m}$ ; (C) enlargement of lower left portion of specimen showing multi-layered body wall. Scale bar = 20  $\mu\text{m}$ .

A series of specimens which together illustrate the result of progressive pyritization is shown in Figure 6. Figure 6A shows a specimen similar to that seen in Figure 5, but with a significant portion of the interior containing micrite of the same character as that in the surrounding rock. Figure 6B shows a specimen in which the wall has been heavily pyritized and with pyrite filling a small portion of the interior. The specimen illustrated in Figure 6C has clusters of pyrite grains filling much of the interior. In this regard it is quite similar to a specimen of *Tasmanites* sp. A illustrated by Winslow [56] which also contains pyrite globules in its interior [56] (Plate 20, Figure 7). Following Grey and Willman [57] such clusters may represent infestations of microbes concentrated on cell degradation products within the vesicle, including sub-cellular organelles and reproductive spores as suggested by Kaźmierczak and Kremer [26]. The specimen in Figure 6D retains an outer halo of sparry calcite crystals, but most of its interior is filled with a solid mass of pyrite. It closely resembles the pyritized Ediacaran acritarch illustrated by Grey and Willman [57] (Figure 4A), or the Devonian specimen of *Tasmanites sinuosus* illustrated by Winslow [56] (Plate 20, Figure 3). Only near the white arrows in Figure 6D is the body wall visible. Many small masses of pyrite project outward from the surface of the pyrite fill. These projections seem far too irregular in shape to have replaced original spines. They may be pyrite crystallites that have overgrown the pyrite fill. Alternatively, they resemble tiny grains of pyrite dispersed within the hollow spines of *Dicrospora multifurcata* illustrated by Winslow [56] (Plate 13, Figures 1–6), and thus may represent pyrite grains in which the surrounding spines are now lost. Where the vesicle wall is visible, it appears to be a simple single walled structure typical of the wall associated with the *Tasmanites*-complex of microalgae. However, punctae are not visible.

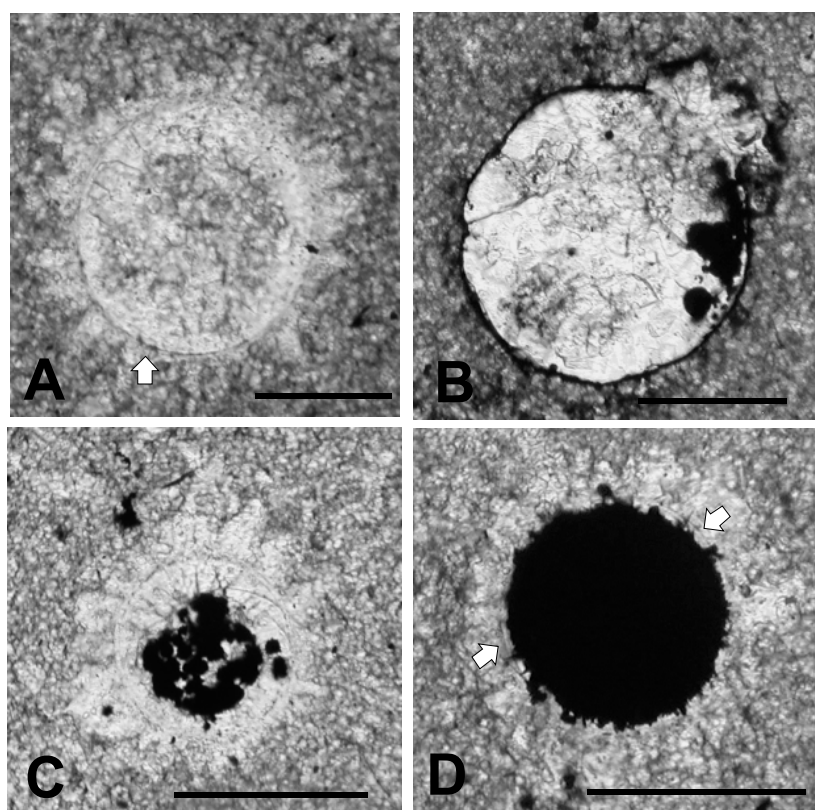


**Figure 6.** Microalgae in thin section showing progressive degrees of pyritization. All scale bars = 100  $\mu\text{m}$ . (A) specimen (TYT-11) with crystalline calcite halos, as in Figure 4. Micrite fills most of the interior. Body wall is pyritized near white arrow; (B) specimen (TYT-04) with pyritized wall and small masses of pyrite in the central body; (C) specimen (TYT-09) with numerous small masses nearly filling the central body; (D) (TYT-01) specimen nearly totally composed of pyrite but retaining a surrounding halo of calcite crystals. Original, body wall is visible near white arrows.

### 3.2. SEM Results

Specimens extracted from the sediment using the separation technique described above are invariably completely pyritized. To the naked eye and when viewed using a stereozoom light microscope, such specimens resemble smooth-surfaced, ovoid to spherical, metallic pellets. Most have the bright yellow color characteristic of pyrite, but some are reddish orange, and a few are black. Where they occur, spines are apparent as tiny points on the otherwise featureless surfaces. Occasionally, specimens show crystalline masses of pyrite overgrowing a portion of their circumference. Because they are completely free of sediment, the pyritized specimens can be studied in any orientation. One is not limited to cross sections fortuitously revealed in thin section. SEM imaging gives views of surface features impossible to obtain by other means.

#### 3.2.1. Sphaeromorphic Specimens

Several non-spinose, pyritized sphaeromorphs (we use this term to mean a spheroidal specimen lacking prominent surface ornamentation) are illustrated in the SEM images in Figure 7. Many sphaeromorphs, such as those in Figure 7A,C, are actually ovoid rather than spherical in shape, but most are spherical as is the specimen shown in Figure 7B. Figure 7A shows a sphaeromorph that, except for a few small, crater-like pits, has a surface that is relatively smooth and featureless. This surface probably corresponds to the vesicle surface. The pits resemble vesicle surface markings associated with the tubular canals, or punctae, commonly observed in vesicle walls of the prasinophyte microalga *Tasmanites* by Burden et al. [58] (Plate 3.1, and 3.2); Colbath [59] (Figures 9, 10, 13 and 15); and Filipiak [60] (Plates VIII.7 and VIII.9). However, these structures in Figure 7A are rather larger compared to the size of the vesicle than is commonly the case for punctae. Also, relatively few are observed in Figure 7A, whereas punctae, when visible, are usually more numerous than in Figure 7A. However, there is wide variability in tasmanitid punctation, and the features seen in Figure 7A are within this range of variation when compared to the tasmanitid specimen illustrated in Burden et al. [58] (Figure 3.1). In addition, the small, circular pits visible on the specimen's surface appear similar to structures seen in the tasmanitids figured by Colbath [59] (Figures 5–10 and 13–15), and interpreted by him as punctae. We therefore interpret these features in our specimens as punctae.

A specimen with a rough, irregular surface is seen in Figure 7B. This roughened surface appears that lie below the probable surface of the specimen, as indicated in the upper and lower right (white arrows), which itself appears slightly rugose. This interpretation suggests that wall thickness in this specimen is about 25 to 30  $\mu\text{m}$ . Such finely rugose specimens are also common. They may represent specimens in which only irregularly pyritized regions of the vesicle wall are preserved. In this regard, they bear some similarity to tasmanitids having surfaces roughened by the impressions of mineral grains illustrated by Colbath [59] (Figure 7).

The sphaeromorph illustrated in Figure 7C has a surface consisting largely of a mosaic of pseudopolygonal "tiles" separated from one another by narrow cracks. The reticulated surface pattern is reminiscent of that associated with members of the genera *Dictyotidium* and *Cymatiosphaera*. However, in these genera reticulation is the result of small ridges or crenulations elevated above the vesicle surface; it is not due to cracks as in the specimen illustrated in Figure 7C. The tiles are also similar to polygonal platelets occurring in the wall structure of the Proterozoic microalga *Dictyosphaera macroreticulatus* described by Agić et al. [61] (Figures 3 and 4). However, dictyosphaerid platelets have straight, linear edges and are therefore much more regularly geometric in their shape, than the tiles illustrated in Figure 7C. A thin, fine-grained covering is draped over the cracked surface visible in the upper left (white arrow) of Figure 7C. This material extends across the top and right side of the specimen and itself becomes progressively more intensely cracked toward the specimen's equator (white arrow). We tentatively interpret this tiled surface topography as the result of vesicle expansion associated with post-mortem mineralization of the vesicle wall. It is not in our view, an inherent part of the wall structure of the specimen, as is the case with dictyosphaerid platelets.

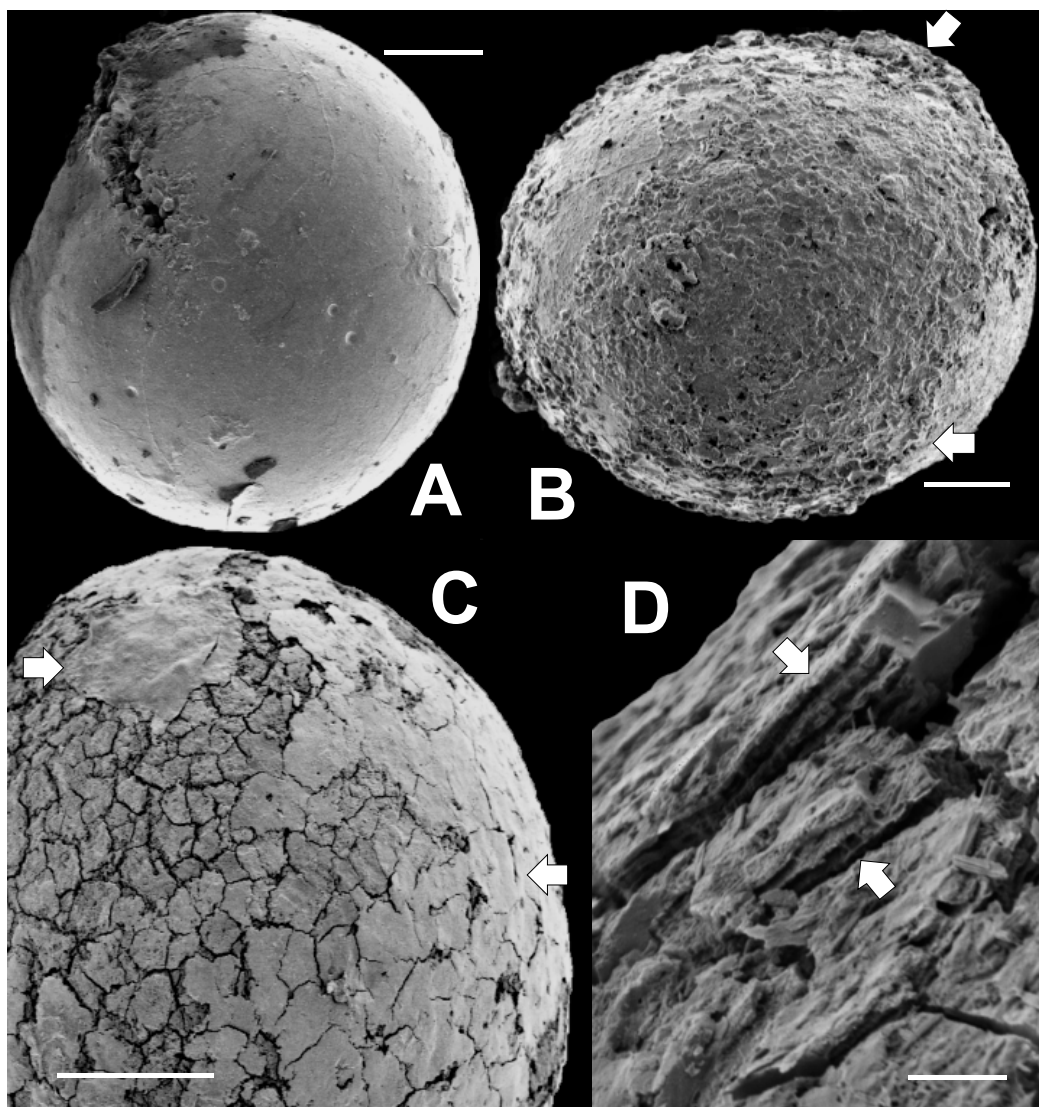


**Figure 7.** SEM images of non-spinose, sphaeromorphic pyritized microalgae extracted from rock matrix. Scale bar in A, B, and C = 50  $\mu\text{m}$ . Scale bar in D = 5  $\mu\text{m}$ . (A) specimen (TYS-14) with smooth surface split open in upper left; (B) specimen (TYS-02) with smooth surface covering small portions of upper right and lower left quadrants. White arrows indicate locations where smooth regions overlie the roughened area at the center of the specimen; (C) specimen (TYS-23) with a surface composed of pseudopolygonal “tiles” overlain in upper left (white arrow) by a thin, smooth, fine-grained covering. This covering becomes progressively broken into tiles toward the lower right (white arrow); (D) Close-up of tiled surface of TYS-23 in cross-section showing that this surface consists of several thin parallel layers 1 to 2  $\mu\text{m}$  thick. In places, (white arrows) narrow, columnar or pillar-like structures extend between the layers.

A close-up of a small portion of such a tiled specimen showing surface structure in cross-section (white arrows) appears in Figure 7D. It appears from this figure that the surface is underlain by a series of thin layers 1 to 2  $\mu\text{m}$  thick. There are at least six of these layers. Their spacing is similar to the laminations seen in the vesicle wall of *Tasmanites somneri* [56] (Figure 12). In places, these layers are only partly filled by solid material. Near the white arrows in Figure 7D the layers appear to be connected by very thin, vertically oriented septa-like partitions one to two micrometers apart. These structures are too planar, and too closely spaced to be punctae. In addition, they lack the pitted surface expression one would expect to see if they were punctae.

Specimen 7A is split open at the upper left. Small pyramidal crystals can be seen filling the opening. Such splits are not uncommon in the material we have examined. The long, linear aspect of these ruptures, as in Figure 7A, suggests that they are probably lateral excystment openings as described by Colbath and Grenfell [22] and Strother [62]. The other alternative, that they are cracks developed during post-mortem mineralization of the vesicle wall, seems considerably less likely to us. The reason is that post-mortem, mineralization-related cracking produces the pseudopolygonal, tiled pattern seen in Figure 7C,D. The parallelism between this pattern and that of mud cracks created when fine-grained sediment dries out is apparent. It is also telling because the polygonality of mud crack development is the result of small, point-like cracks initiated more or less contemporaneously, propagating with continued drying until they intersect with, and are stopped by, other cracks growing nearby. Because there are a multitude of nucleation points at which cracks can begin in homogeneous materials like fine grained sediment, no crack can extend very far before it is stopped—hence the pattern. The organic walls of algal and acritarch vesicles are also nearly uniform compositionally and structurally, and consequently post-mortem mineralization nucleates in a multitude of sites as suggested by the large number of tiny, dark, closely spaced pyrite grains seen in specimens in which mineralization is still in an incipient state (Figures 5B,C and 6A). Due to this close spacing, as mineralization progresses in the vesicle wall, cracks can propagate only a very small distance, a few micrometers at most, before being stopped by adjacent cracks. Thus, long, linear splits like those in Figure 7A, could not be related to mineralization. They must have formed prior to it. They are most likely excystment scars.

### 3.2.2. Acanthomorphic Specimens

SEM images of four acanthomorphic pyritic specimens are given in Figure 8. They closely resemble the pyritized acanthomorphic acritarchs figured by Loydell et al. [14] from Ordovician black shales of the Welsh Borderlands. The spines seen in Figure 8 are typical of all material examined so far. Figure 8A shows a spheroidal specimen with a large crack in the lower right quadrant and with missing material near the left end of the scale bar. We interpret this rupture as a lateral excystment opening as described by Strother [61]. The spines are conical in shape, spaced about 20  $\mu\text{m}$  apart, and arranged in a regular array. The ovoid specimen in Figure 8B shows spines of a similar character. Figure 8C,D are close-ups of small portions of two other specimens. The spines illustrated in these two figures are 20 to 30  $\mu\text{m}$  high. A few taper gently to a sharp tip, but most have flat tops. Some flat-topped spines are shorter than sharp-tipped ones, and thus probably represent spines with their tips broken off. Most spines appear to have solid interiors, but a few (white arrows in Figure 8C,D) are hollow. These hollow spines probably represent the original condition of the spines when the organisms were alive. There is no indication in any of the specimens we studied of distal spine bifurcations. However, a few spines, such as the one highlighted by the white arrow in Figure 8C, have tips with a narrow, flared, flat rim. These flared tips are considerably smaller, and less ornate than the prominent flared spine terminations seen in some specimens of *Dicrospora* [56] (Plates 10–13), *Puteoscortum* [63] (Plate 1), *Peteinosphaeridium* [64] (Plate 4, Figure 4), or *Multiplicisphaeridium* [64] (Plate 5, Figure 7).

### 3.2.3. Crystallinity of Extracted Specimens

An SEM image of an incompletely preserved sphaeromorph is shown in Figure 9A. It probably represents a calcitic sphaeromorph originally containing a large internal mass of pyrite similar to the specimen in Figure 6C but with the pyrite concentrated in one hemisphere, and in which only this pyritic portion survived the extraction process. Such hemispherical specimens are not uncommon, and are similar to the pyritized ‘half-spheres’ of Schieber and Baird [16] (Figure 2). Figure 9A indicates that the Tully half-sphere is filled with a mosaic of interlocking euhedral pyrite crystals, most of which are about 10  $\mu\text{m}$  in size, but including some larger ones as well. When viewed in more detail (Figure 9B), the specimen is seen to contain numerous small framboidal clusters of pyrite less than 1  $\mu\text{m}$  in size mixed in with the larger euhedral crystals of pyrite. In some cases, pyrite framboids are an abundant

sphaeromorph constituent, as in Figure 9C, where frambooids cover the surface of a large ovoid space in the interior of another smooth specimen. Hollow sphaeromorphs, such as the specimen illustrated in Figure 9C, are also described by Schieber and Baird [16] (Figure 4A). Rarely, as in Figure 9D, ovoid frambooids can be found attached to the outer surface of a sphaeromorph. These are essentially identical to pyrite structures described by Grey and Willman [57] as bacterial infestation scars on the body wall in their Neoproterozoic acritarchs. Figure 9E shows an acanthomorphic specimen with a fine-grained outer covering, either incompletely formed, or partially ripped open. The interior of the specimen is filled with euhedral pyrite crystals similar to those seen in the smooth-surfaced specimen in Figure 9A. One also gets a sense from Figure 9, that the interior of Tully pyritic specimens contains much open space, either as large voids (Figure 9C), or as smaller gaps between the euhedral grains (Figure 9E). Figure 9F is an EDX spectrograph of the fine grained surface covering of the specimen X-rayed at the point indicated by the star in Figure 9E. The spectrograph in Figure 9F is typical of all EDX spectrographs obtained for the 10 specimens we X-rayed. The major peaks are those of iron and sulfur. Thus, it appears that the fine material comprising the surface of the specimen is also pyrite.

#### 3.2.4. Deformed Specimens

A specimen, similar to those illustrated in Figure 6B,C in having a heavily pyritized wall and internal pyrite masses is shown in Figure 10A. In addition, sparry calcite fills the interior not occupied by pyrite, and a partial internal halo of elongate calcite crystals lines a portion of the inner wall surface. However, in its non-circular shape, this specimen differs significantly from the specimens illustrated in Figure 6B,C. The wall is broken in two places (noted by arrows in Figure 10A), and the smaller piece thus formed, appears to have shifted downward and to the left relative to the remainder of the specimen. This separated piece is curved inwardly, i.e., it is convex toward the specimen interior rather than bowed convexly outward. The unusual condition of this vesicle is consistent with the idea that the specimen's thin wall was bent inward while the wall was still flexible. Subsequently, authigenic growth of sparry carbonate crystals may have caused the vesicle to split open and to separate the remnants, probably after the wall was pyritized. Figure 10B,C show SEM images of two other specimens. These specimens have intact, unbroken walls, but it is evident that they too have walls that have been depressed inward to a significant degree. The folding of the wall in Figure 10C is especially intense, and illustrates the high degree of flexibility these specimens retained during at least part of the preservation process.

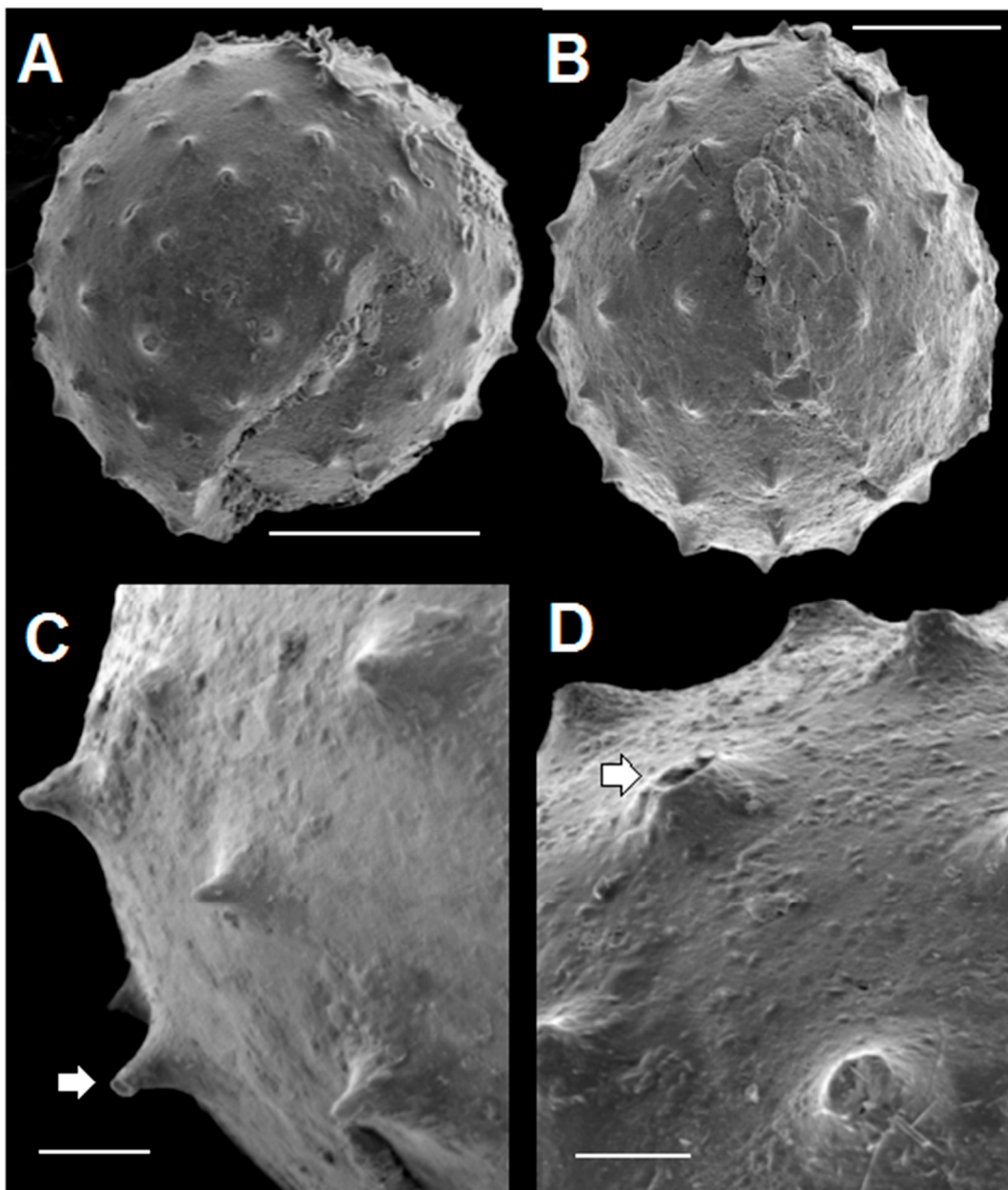


**Figure 8.** SEM images of pyritized spinose, acanthomorphic specimens extracted from rock matrix. Scale bar in A = 40  $\mu\text{m}$ . Scale bar in B = 25  $\mu\text{m}$ . Scale bar in C, D = 10  $\mu\text{m}$ . (A) spheroidal specimen (TYS-29) with large crack showing arrangement of spines; (B) ovoid specimen (TYS-38) with spines; (C,D) Detail of spines in two specimens. White arrows point to flat-topped spines that have hollow interiors. C: TYS-32. D: TYS-41.

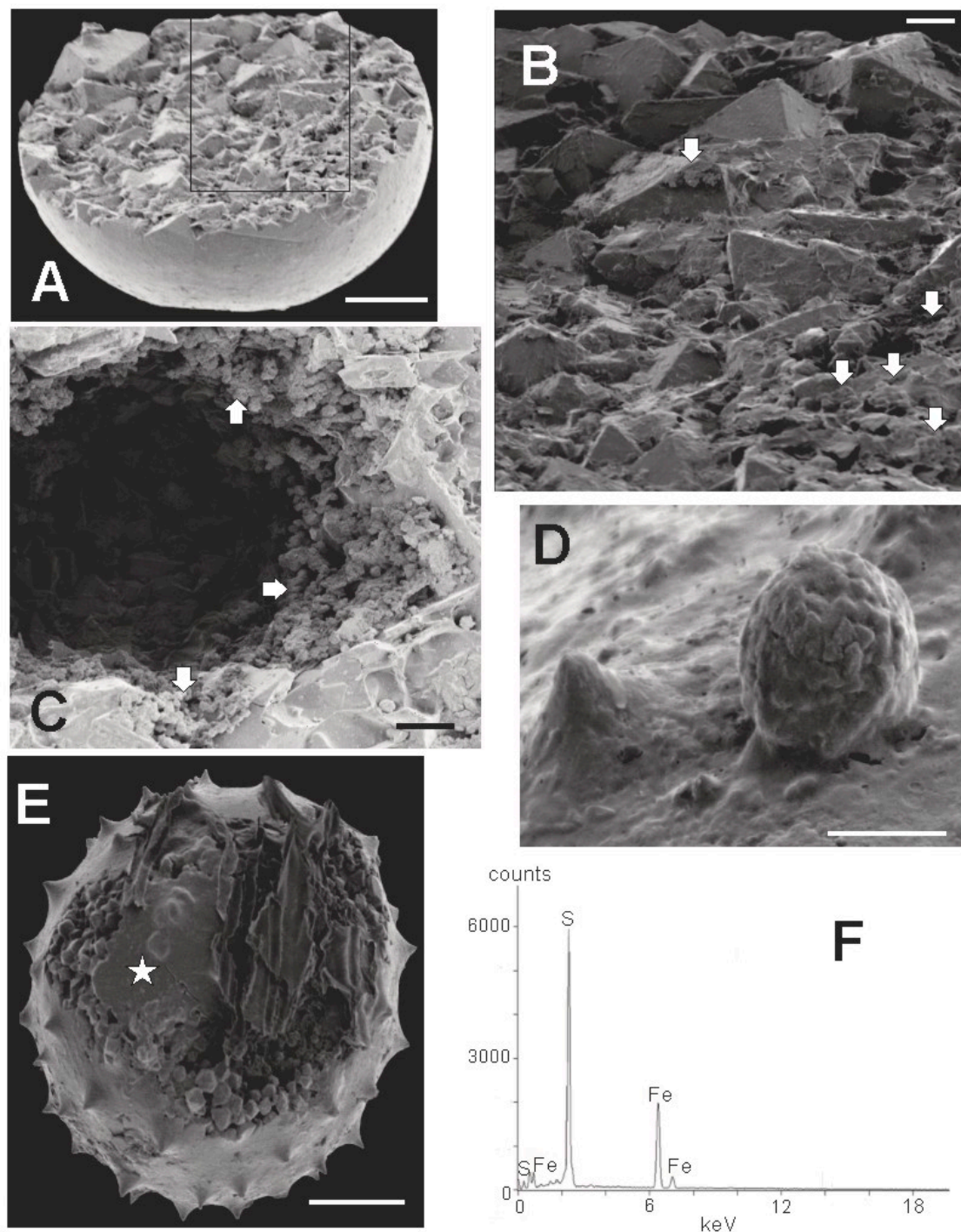


**Figure 9.** Composition of specimens extracted from rock matrix. Scale bar in A = 50 μm. Scale bar in B: 10 μm. Scale bar in C, D = 5 μm. Scale bar in E = 20 μm (A) SEM image of incompletely preserved sphaeromorphic specimen (TYS-16) showing an interior filled with cubic and pyramidal crystals of pyrite. Box outline is the perimeter of the enlargement shown in B; (B) Detail of crystalline surface showing large euhedral pyrite crystals and smaller pyrite framboids (white arrows); (C) Detail of a large open space within the interior of a sphaeromorphic specimen (TYS-17) showing clusters of framboids lining the space (white arrows) and large euhedral crystals at the bottom of the opening; (D) Spheroidal framboid with individual crystallites of 1 μm or less growing from the surface of an acanthomorphic specimen (TYS-45); (E) Acanthomorphic specimen (TYS-41) filled with euhedral pyrite crystals. Star shows the target area of the x-ray beam producing the spectrograph illustrated in F; (F) X-ray signature of smooth surface at position of star in E. Main peaks are those of iron and sulfur.

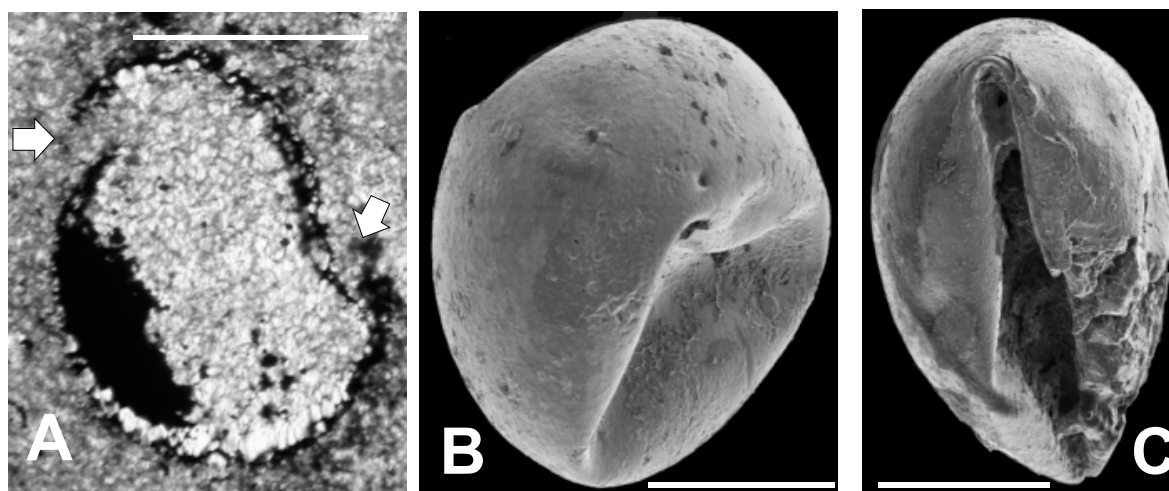


**Figure 10.** Deformed specimens. Scale bar in A, B, and C = 100  $\mu\text{m}$ . (A) Thin section of a specimen (TYT-11) with a portion of the body wall split away from the main body. The fragment has an inwardly convex curvature; (B) SEM image of a sphaeromorphic specimen (TYS-15) with an inwardly convex depression in its body wall; (C) SEM image of a sphaeromorphic specimen (TYS-04) with a sharp, crease-like fold in its body wall.

### 3.2.5. Surface Covering

Many of the specimens, particularly spiny ones, have a thin covering of fine grained, material, about 0.5  $\mu\text{m}$  thick, which frequently appears to have split open and then peeled away from the vesicle surface in elongate rolls, as is evident in Figure 11A. This material, and the manner of its separation from the vesicle surface, superficially resembles the torn outer wall of a *Velatasphaera hudsonii* specimen figured by Miller and Williams [65] (Plate 2). However, in our specimen the torn material, where it is not ripped up, adheres to the surface of our specimen, including the spines, as is seen in Figure 11A,B, whereas in *V. hudsonii* the torn material represents a rugose sheet propped up on the tips of the spines [65] (Plates 2.2, 2.3, 2.4) At higher magnification, this thin surface layer in our specimen (Figure 11A–C) is seen to contain numerous shallow, circular and ovate pits, resembling collapsed air bubbles (Figure 11B). This is unlike the torn sheet observed in *V. hudsonii*, which is devoid of such pits. The pits are also not punctae, as they penetrate only the half micrometer thick surface sheet (Figure 11B), a structure much too thin to represent the vesicle wall. Although extremely thin and fine grained, in places this surface material shows faint, rhombic patterns which may represent rhombs of thin pyrite crystallites (Figure 11B). We interpret this surface material as the preserved, and now pyritized, remains of a mucilaginous sheath or membrane surrounding the living cell. Such gelatinous envelopes occur widely among modern green algae [66–69]. The pits, in our view, are the result of the escape of gas bubbles produced by the decomposition of organics in the mucilaginous sheath or in the vesicle wall itself during the earliest phases of post-mortem decay.

An acanthomorph that has split open revealing euhedral pyrite crystals within is illustrated in Figure 11C. These crystals have rounded and muted edges and corners. In a few places, rounded pits similar to those in the pyritized mucilaginous material covering the surface of the specimen, and visible in the lower right and upper left, are present in the crystalline area as well. It is evident from Figure 11C that this surface material is draped over the exposed interior crystals as well as adhering to the specimen surface. This is a clear indication that the pits are not punctae. It also suggests that the surface layer was present when the vesicle filled with authigenic pyrite and coated the outermost of these crystals as they enlarged, or that the surface layer mineralized after the split had occurred. Either scenario is consistent with the idea that this surface layer is the remains of a pyritized mucilaginous membrane.

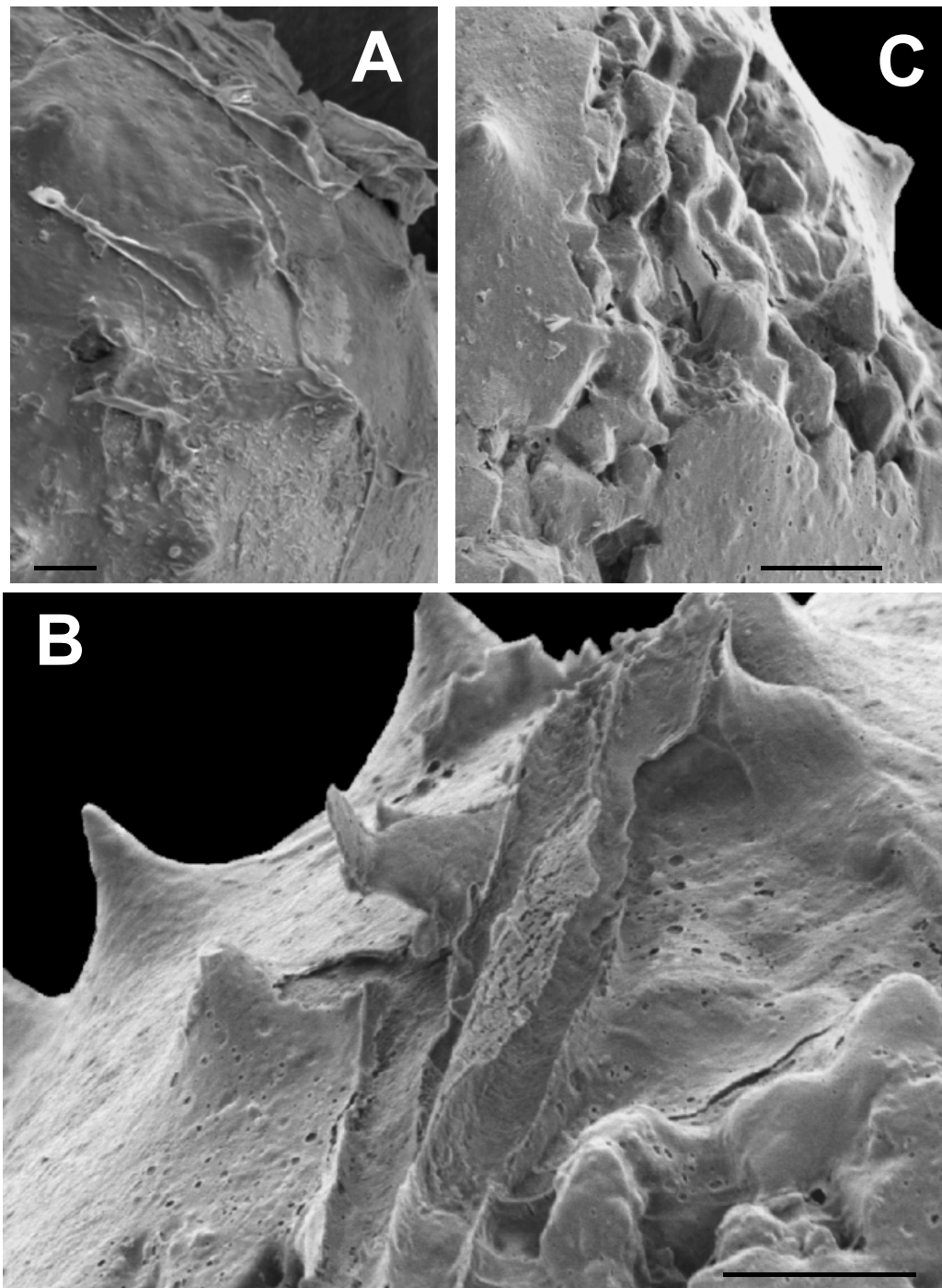


**Figure 11.** Microalgae having a thin, coating or layer at the surface. All scale bars = 10  $\mu\text{m}$ . (A) SEM image of an acanthomorphic specimen (TYS-40) having a thin surface layer which has split away from the surface. The edges of this layer turn up, and in places form long tube-like rolls; (B) SEM image of an acanthomorphic specimen (TYS-51) showing that this layer contains numerous ovate or circular pits similar in appearance to collapsed air bubbles; (C) SEM image of an acanthomorphic specimen (TYS-44) which has split open revealing pyrite crystals within the interior. A well-developed thin, pitted layer is visible covering the surface of the specimen at the lower right and upper left, and extending across the tips and exposed surfaces of the interior crystals.

#### 4. Systematic Paleontology

In this section we describe and identify microfossil taxa found in the Lower Tully Formation at Lock Haven. In the course of this study, we examined several hundred individual pyritized microalgae and acritarchs, and use these specimens as a basis for the formal systematic treatment of algae and acritarch taxa that we present here. In contrast, microorganisms that co-occur with the microflora are relatively few in number and are insufficient to obtain an understanding of their morphological attributes sufficiently robust to support formal taxonomic treatment. Consequently, we present only an informal identification of them here.

##### 4.1. Algae and Acritarchs

Finding taxonomic homes for algae and acritarchs of Paleozoic age has been a controversial process. Nevertheless, in the last two decades, great strides have been taken in improving systematic associations of many Paleozoic organic-walled microfossils. Three advances seem particularly relevant. First is the recognition that the mineralogy of these fossils is a post-mortally induced feature and does not, therefore, have major taxonomic significance. Thus, muellerisphaerids are not a separate group of originally phosphatic spherical microorganisms, as conceived by Kozur [12]; they are actually originally organic-walled microorganisms that have been preserved through a process of rapid, post-mortem phosphatization [2,18]. Second, it is now clear that subcellular structures, which are often useful in classifying microscopic eukaryotes, can be preserved via a variety of different post-mortem preservation pathways including silicification [27] and pyritization [26,27,57]. Thus, some acritarchs with preserved internal bodies can be recognized as the sporulating vegetative cells of unicellular chlorococcalean green algae [26,27]. Finally, specific biomarker compounds contained in the walls or cytoplasm of microorganisms, or their post-mortem decompositional derivatives, can now be used to aid taxonomic work on microfossils [70–74]. Thus, steranes can be used to help identify the presence of prasinophyte green algae in rocks of Neoproterozoic and Paleozoic age [73], although it is not yet possible to use this approach to identify specific prasinophyte specimens. Study of biochemical properties is becoming an increasingly valuable means of circumventing taxonomic difficulties deriving from morphological convergence among potentially widely different taxa [28].

Organic walled microorganisms, like large organisms, are subject to post-mortem degradation that can modify, or obliterate, characters that are taxonomically significant [57] (and references therein), and thus hinder attempts to properly classify them. The Tully material has clearly undergone considerable post-mortem alteration. Tully specimens are calcified and pyritized; deformed; and with ornament and sub-cellular microstructures almost entirely eradicated or highly modified as a result. Moreover, since the Tully material is composed now of calcite and pyrite, sophisticated biochemical approaches that have proven effective in specimens preserved in siliciclastic rocks, and particularly in microcrystalline cherts, have limited applicability at best with respect to the specimens described here.

Another current problem for the taxonomy of fossil acritarchs and algae is the growing awareness [28,74] that morphologically distinct organic-walled microfossils may actually represent different ontogenetic phases in the complex life cycles characterizing many unicellular eukaryotic organisms, algae in particular. Thus, acritarch or fossil algal specimens that have been referred to different taxa may actually be different developmental stages of the same species. Compounding this situation is that recent study of eukaryotic genomes and ultrastructure has produced a wide difference of opinion on appropriate higher levels of eukaryotic taxonomy [75–79]. Because of the current fluidity in the status of higher level designations for green algae, and because we recognize no new species, we use an abbreviated format in synonymizing our taxa. We follow Moczyłowska et al. [28] in considering tasmanitids as algae rather than as acritarchs. We also follow the systematic scheme for green algae proposed by Adl et al. [76].

Our identification of only three species (two algae and one acritarch species) in our material contrasts markedly with the much greater diversity of algae and acritarchs seen in other Devonian microfloras of the Appalachian and associated basins (e.g., 10 species in the Upper Devonian-Lower

Mississippian section of Ohio [56]; 19 species in the Lower Devonian Kalkberg Limestone of New York [80]; 26 species in the Givetian Boyle Dolomite of Kentucky [81]). This situation with our material may be artifactual in the sense that our restrictive rock sampling regimen under-represents true Tully diversity, or that the loss of taxonomically significant morphologic and biochemical details resulting from post-mortem mineralization of the Tully microfossils masks a wider actual diversity. Knoll and Golubic [82] discuss this problem with respect to Neoproterozoic algal stromatolites. Alternatively, the apparent low Tully diversity may give a realistic reflection of the narrow microfloral diversity often associated with some deep water, offshore depositional settings, as discussed below.

#### 4.1.1. Descriptive Systematics: Algae

Super-group: Archaeplastida Adl et al. [76]

First Order Subdivision: Chloroplastida Adl et al. [76]

Second Order Subdivision: Prasinophytae Cavalier-Smith [83], emend. Lewis and McCourt [75]

Order: Pterospermatales: Tappan [84]

Family: Tasmanitaceae: Tappan [84]

Genus: *Tasmanites*: Newton [85] emend. Schopf, Wilson and Bentall [86]

Type Species: *Tasmanites punctatus* Newton [85]

Remarks: *Tasmanites* is a common microalga with representatives known from the Proterozoic [87,88] to the modern ocean [89]. Fensome et al. [90] and Mullins et al. [91] list in excess of 80 and 90 species respectively. Of these, Fensome et al. [90] indicate that 28 species are Devonian in age. Six of these (*T. asper*, *T. decorus*, *T. huronensis*, *T. sinuosus*, *T. sommeri*, and *T. winslowiae*) are Middle Devonian species with geographic ranges that include the western reaches of the Appalachian Seaway (Ohio, Illinois, Ontario) [92]. None, however, are known to occur as far eastward as the north-central Pennsylvania Tully locality discussed here.

*Tasmanites* has a smooth or rough-surfaced sphaeromorphic form lacking strong spines or other well-developed ornamentation. Members of this genus have diameters generally ranging between 40  $\mu\text{m}$  and 500  $\mu\text{m}$ . *Tasmanites* is characterized by a simple one layered wall, usually quite thick relative to vesicle diameter, i.e., 10% or greater, but some species are known to be thin-walled, i.e., with walls about 5% vesicle diameter. In some species, the vesicle wall shows fine, concentric laminations. The vesicle wall is also characterized by small, radially oriented, tubular canals termed punctae. Punctuation is variable in spacing and prominence, and is not always visible. Excystment is by means of a linear split. The Tully material illustrated here contains several specimens which we assign to the genus *Tasmanites* on the basis of vesicle size and morphology, wall structure, excystment pattern, and punctuation.

*Tasmanites*. cf. *T. sinuosus* Winslow [56]

Specimens in Figures 6A–D and 10B

Remarks: According to Winslow [56], who first recognized and named *T. sinuosus*, this species is characterized by having spherical vesicles 50 to 400  $\mu\text{m}$  in diameter with smooth or slightly rugose surfaces. The vesicle wall is punctate, unlaminate, and 2 to 13  $\mu\text{m}$  thick. Characteristics associated with the macerated specimens Winslow [56] studied, e.g., appearance in polarized and reflected light, do not occur in the mineralized specimens discussed here. Winslow [56] indicates that the occurrence of *T. sinuosus* is limited to the Upper Devonian, but Wicander [92] extends its range downward into the Middle Devonian.

Material: Five well preserved partially to completely pyritized specimens (those referred to above in Figures 6A–D and 10B). Mean diameter = 145  $\mu\text{m}$ ; std. dev. =  $\pm 42.25 \mu\text{m}$ .

Description: The four specimens illustrated in Figures 6 and 10B have diameters averaging about 150  $\mu\text{m}$ . Of the six Middle Devonian Appalachian Seaway tasmanitid species listed above, only *T. sinuosus* has vesicles as small as these Tully tasmanitid specimens. In addition, the specimens illustrated in Figure 6, have simple vesicle walls, which although thin compared to most tasmanitids (about 5% vesicle diameter), lie within the range of wall thickness Winslow [56] attributes to *T. sinuosus*. The deformed specimen seen in Figure 10B has several large punctation pits. We thus suggest that these five specimens most closely resemble *T. sinuosus*. The specimen illustrated in Figure 5 has a diameter of about 150  $\mu\text{m}$  and therefore is small enough to be *T. sinuosus*, but it also has a laminated wall. This would exclude it from this species because Winslow [56] very clearly indicates that *T. sinuosus* has a simple, un-laminated wall. Study of additional Tully material, particularly specimens prepared by maceration, is required to provide a firm species designation for these specimens.

Tasmanites. cf. *T. sommeri* Winslow [56]

Specimens in Figures 5 and 7A–D

Remarks: Winslow [56] diagnosed this species as having nearly circular vesicles 320–550  $\mu\text{m}$  in diameter. Wall thickness is 30–70  $\mu\text{m}$  and increases with increasing diameter. Vesicle walls are punctate and often laminated with as many as 10 to 12 individual dark laminae separated by about 3–5  $\mu\text{m}$ . Punctae are described as being numerous with a tapering, tubular shape, and usually separated from one another by about 25 to 30  $\mu\text{m}$ . Optical properties noted by Winslow [56] in macerated specimens are not present in the mineralized specimens discussed here. Winslow [56] indicates that *T. sommeri* is limited to the Upper Devonian Olenitangy Shale and lower Ohio Shale, but Wicander [92] extends its range downward into the Middle Devonian.

Material: Five well preserved partially to completely pyritized specimens (those referred to above in Figures 5 and 7A–D). Mean diameter = 386  $\mu\text{m}$ ; std. dev. =  $\pm 170 \mu\text{m}$ .

Description: The specimens illustrated in Figure 7A, B, and C have diameters in the range of 400 to 500  $\mu\text{m}$ , which puts them within the lower end of the size range of *T. sommeri*. The specimen in Figure 7A has several shallow pits which we interpret as the surface expression of punctae in the vesicle wall. If so, this specimen appears to be punctate as described above, and also exhibits a linear excystment split typical of tasmanitids. Figure 7D indicates that tiled specimens like that in Figure 7C, have a vesicle wall consisting of many fine laminations, a key characteristic of *T. sommeri*. Although we consider the specimens in Figure 7 to resemble individuals of *T. sommeri*, it seems obvious that study of more, and particularly of macerated, specimens is needed to confidently identify this taxon among Tully sphaeromorphs. The specimen illustrated in Figure 5, has a laminated wall, but only one such lamination is clearly seen. However, additional laminae are visible over short distances at several points around the vesicle (e.g., upper left corner of Figure 5), so we tentatively include this specimen in this designation also.

#### 4.1.2. Descriptive Systematics: Acritarchs

Group: Acritarcha Evitt [20]

Subgroup: Acanthomorpha Downie, Evitt and Sarjeant [93]

Genus: *Solisphaeridium* Staplin, Jansonius and Pocock [94], emend. Sarjeant [95]

emend. Moczyłowska [96]

Type species: *Solisphaeridium stimulierum* Deflandre [97]

Remarks: *Solisphaeridium* is a common acritarch with representative species known from the Cambrian [98,99] to the Paleocene [100]. However, the genus appears to be most diverse in the Ordovician. Fensome et al. [90] and Mullins et al. [91] list in excess of 26 and 23 species respectively. Of these, Fensome et al. [90] indicate that six species are Devonian in age. One as yet indeterminate

species of the genus occurs in the Lower Devonian Kalkberg Limestone of New York State [80] and *S. spinoglobosum* occurs in the Upper Devonian of Ohio [101]. *Solisphaeridium laevigatum* occurs in the Givetian of Iowa [102]. However, no *Solisphaeridium* material has yet been reported from the Middle Devonian of New York or Pennsylvania.

*Solisphaeridium* (?)

Specimens in Figures 8, 9D–E, 11 and 12

Remarks: *Solisphaeridium* is a genus of acanthomorphic acritarchs characterized by vesicles with a spherical or subspherical shape. Typically, vesicle diameter is in the range of 20 to 40  $\mu\text{m}$ . The genus is characterized by specimens having numerous relatively long, slender spines which widen toward their base. The spines are hollow and open directly into the vesicle interior. Excystment is by means of a linear split, or by loss of a small piece of the cyst wall.

Material: Five pyritized specimens (those referred to in Figures 8, 9D–E, 11 and 12). Mean diameter of three measured specimens (Figures 8A,B and 9E) = 96  $\mu\text{m}$ ; std. dev. =  $\pm 7.5 \mu\text{m}$ .

Description: Taken together, the acanthomorphic Tully specimens listed above possess attributes characteristic of *Solisphaeridium*. They are spherical to subspherical in shape (Figures 8, 9 and 11), with excystment by means of linear splitting of the vesicle wall (Figure 8A), and with spines widening gently toward their base (Figures 8, 9 and 11). Although most spines are filled with secondary pyrite crystal growth, the Tully specimens have what we interpret to be hollow spines (Figure 8C,D) which we argue was the original spine condition prior to post-mortem mineralization. The shape and spacing of the spines in the Tully specimens is also a feature typical of some species of the genus. Examples include the Upper Devonian *S. spinoglobosum* [101] (Plate 6, Figures 1 and 2); [102] (Plate 6, Figures 1 and 2); the Middle Devonian *S. laevigatus* [103] (Plate III, Figures 2 and 3); the Cambro-Ordovician *S. akrochordum* [99] (Plate 13, Figures 1–6); and the Jurassic *S. brevispinosus* [104] (Plate 2, Figure 8). In addition, there is evidence that the cavity inside the spines opens directly into the vesicle interior. Figure 12 shows a spine in which the growth of pyrite crystals within the spine does not appear to be inhibited by the presence of a partition or vesicle wall, as would be the case if spines were closed off at their base. Since vesicle walls and laminae within vesicle walls are readily pyritized and preserved in the Tully specimens (Figure 7D), the absence of a pyritized partition at the base of this spine (Figure 12B) is consistent with the view that this spine was probably not blocked off at its base when the organism was alive. Many Paleozoic acanthomorphs have spines which superficially resemble the spines exhibited by our specimens (e.g., *Gorgonisphaeridium*, *Lophosphaeridium*, *Buedingisphaeridium*; *Baltisphaeridium*), but only *Solisphaeridium* is noted for having hollow spines open to the vesicle interior.

Although the observations outlined above suggest that the Tully acanthomorphs belong to the genus *Solisphaeridium*, we do not think that the evidence is strong enough to be confident in this assignment. There are several issues here. First, *Solisphaeridium* generally has longer spines relative to the size of the vesicle than is the case with the Tully acanthomorphs. Secondly, the spine illustrated in Figure 12 is the only example we have yet observed where the interior of the spine at its juncture with the body can be observed. More examples would be needed to make the assertion of direct spine communication with the vesicle interior more confidently. Finally, vesicle diameter in the Tully specimens is considerably larger than that characteristic of *Solisphaeridium*. Further work, particularly with specimens processed via maceration would be useful in resolving these issues, and placing this assignment on firmer ground.

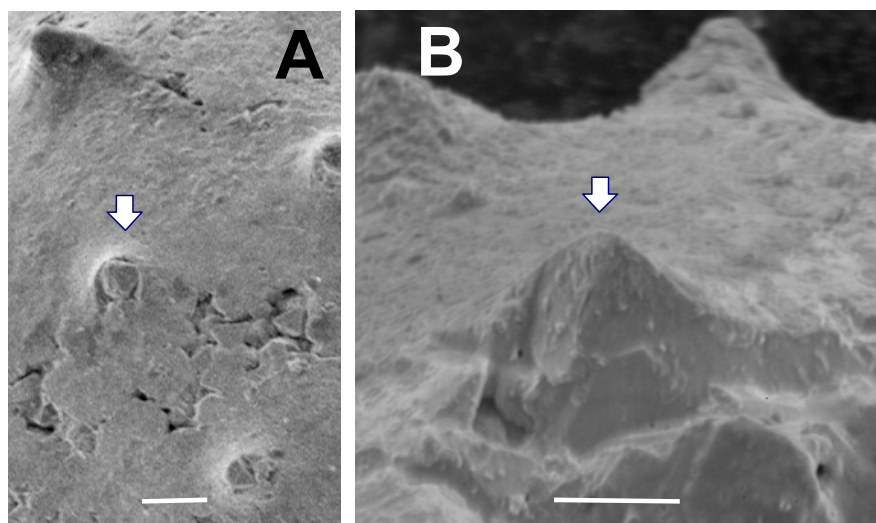


**Figure 12.** Close-up of several spines of a Tully acanthomorph (TYS-43). Arrows point to the same spine in both A and B. (A) Spines viewed from directly above vesicle surface. Spine indicated by arrow contains a stack of large pyrite crystals growing up from vesicle interior. Scale bar = 10  $\mu\text{m}$ ; (B) Close-up of this spine shows the open spine interior filled with pyrite crystals inside it, and with no obvious vesicle wall or partition within the spine. Scale bar = 10  $\mu\text{m}$ .

## 5. Co-Occurring Organisms

The algal and acritarch cells discussed in this paper occur as part of a microbiota, first reported by Brown et al. [105] and Chamberlain and Brown [106], which also consists of molluscs, ostracodes, ctenostome bryozoans, dacroconarids, and the enigmatic microfossil *Jinonicella*. These organisms are preserved in the same way as the algal and acritarch cells themselves, i.e., as partially or completely pyritized steinkerns. Figure 13 shows pyritized examples of the main constituents of this microbiota. None of these organisms are larger than about 1.5 mm in the longest dimension. We did not systematically measure size in this material for several reasons. In some cases we only recovered a single specimen per taxon in which case size is given adequately by the scale bars in Figure 13. In others, specimens were too poorly preserved or too incomplete to obtain reasonable length estimates. In such cases we selected the specimens illustrated in Figure 13 to give a representative sense of size. We provide here only tentative, generalized identifications of these micro-organisms. Formal systematic assignments must await more complete collection efforts of the microfossil horizon and more analytic work with these co-occurring organisms as a focus.

### 5.1. Molluscs

Before going further in dealing with members of this group, we should note that we assume that ontogenetic variation in the taxa represented by our specimens is minimal, i.e., that the morphology of the very early juveniles with which we are obviously dealing here is similar to adult morphology upon which the identifications are actually based.

#### 5.1.1. Bivalves

**Material:** Seventeen incomplete and poorly preserved pyritized specimens.

**Description:** The hinge and umbonal area of a small bivalve found in the microfossil horizon is seen in Figure 13A. It clearly has a “piano-key”, taxodont hinge structure, a relatively straight hinge line and an inflated, roughly equivalve shell shape. Given these characteristics, it probably belongs to the genus *Nuculoidea*, and is most similar to the Devonian form, *N. corbuliformis* as described by Bailey [107].

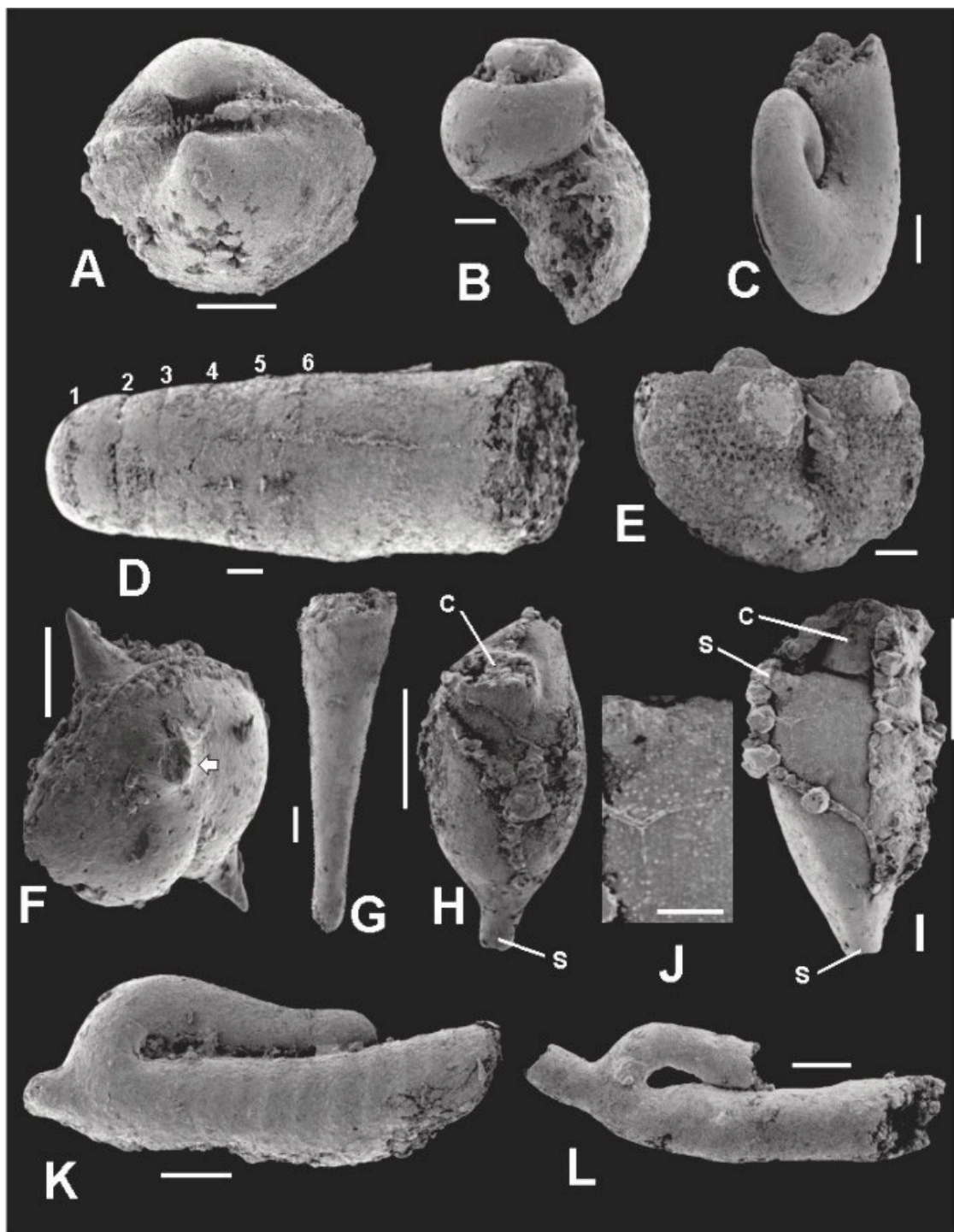


**Figure 13.** SEM images of microorganisms co-occurring with the microflora. Scale bar in J = 40 µm. All other scale bars = 100 µm. (A) TYSV-01; paleotaxodont bivalve, probably *Nuculoidea corbuliformis*; (B) TYSG-01; highspired loxonematacean gastropod, possibly *Palaeozygopleura* sp.; (C) TYSG-02; Euomphalacean gastropod, possibly *Euomphalus* sp.; (D) TYSC-01; Longiconic nautiloid. Numbers identify the positions of the first six septa; (E) TYSO-01; ostracode, probably *Ulrichia* sp.; (F) TYSO-02; spiny ostracode, probably belonging to either to the Aechminidae or Aechminellidae. White arrow points to the base of a broken lateral spine; (G) TYSD-01; Dacryoconarid, probably *Viriatellina* sp.; (H,I) TYSZ-01; TYSZ-02; ctenostome bryozoan zooids. c—collar; s—stolon; (J) enlargement of area at base of lateral stolon in I; (K) TYSJ-01; *Jinonicella kolebabi*, ribbed morph; (L) TYSJ-02; *Jinonicella kolebabi*, unribbed morph.

### 5.1.2. Gastropods

Material: Fifteen incomplete and poorly preserved pyritized specimens.

Description: Two gastropods are shown in Figure 13B,C. The high-spired form in Figure 13B is probably a loxonematacean belonging to the genus *Palaeozygopleura*—most probably *P. hamiltoniae*, which is widespread in the Middle Devonian sequence of New York [108,109]. The nearly planispiral form in Figure 13C is probably a member of the genus *Euomphalus*, also known from the Middle Devonian of the Appalachian Basin [108].

### 5.1.3. Cephalopods

Material: One pyritized specimen.

Description: Judging from its septate, tubular morphology, its small size, and somewhat constricted diameter adoral of the sixth septum, the specimen in Figure 13D is most probably a nautiloid protoconch. The simple concave septa with no sign of a ventral siphuncle weigh against the idea that it is one of the many early ammonoids that are common in Middle Devonian rocks of the Appalachian Basin. Cyrtconic and breviconic nautiloid shells usually show some departure from straightness even in the earliest part of the shell, whereas the shell in Figure 13D does not. Thus, our specimen is most probably a protoconch of a longiconic orthoceratid nautiloid belonging to a species of *Michelinoceras*, *Casteroceras*, *Arkonoceras*, or *Geisonoceras*, all of which occur in the Middle Devonian rocks of eastern North America [110].

### 5.2. Ostracodes

Material: Two pyritized specimens.

Description: The ostracode shown in Figure 13E has a straight hinge, prominent anterior and posterior lobes separated by a deep median sulcus, and a reticulated pattern on the carapace. We consider that it is a member of the genus *Ulrichia*, which has these characters and is known from the Appalachian Middle Devonian [106]. The ostracode illustrated in Figure 13F has a smooth carapace ornamented with prominent medial and lateral spines. It is probably a member of the Aechminidae or Aechminellidae, both of Devonian age [111].

### 5.3. Dacryoconarids

Material: Thirty-one poorly preserved or incomplete pyritized specimens.

Description: A dacryoconarid common in our material is seen in Figure 13G. It has the slightly inflated apical bulb and transverse rings seen among species of the Middle Devonian genus *Viriatellina* [112]. However, the specimens of this form that we have examined so far are all steinkerns and thus do not show external longitudinal costae. Such markings are required for species level identifications for this genus [113].

### 5.4. Bryozoans

Material: Nineteen pyritized specimens.

Description: Two bryozoan zooids partly enclosed by strings and clusters of superficial pyrite crystals adhering to their surfaces are shown in Figure 13H,I. The specimens have the prominent collar and sac-like zoecial shape tapering downward into a basal stolon typical of many stoloniferan ctenostomes. One specimen (Figure 13I) is seen to have the base of a lateral stolon emerging from its distal margin. Figure 13J is an enlargement of the region adjacent to the lateral stolon of the specimen in Figure 13I. Numerous tiny, randomly spaced, irregular protuberances are distributed across the surface of the specimen (Figure 13J). We interpret these structures as micropores, now infilled with pyrite, that originally extended into the outer skeleton surrounding the zooid.

Zoecial shape and stolon arrangement suggest that these specimens may derive from a member of the genus *Ropalonaria*, which have zoaria largely consistent with such features. The shape of the

Tully specimens evident in Figure 13H,I, however, is more inflated than the elongated, fusiform zooecial pits described by Ulrich and Bassler [114] (Plate LVI, Figures 2–11) commonly preserved among species of this genus. In this regard, the Tully specimens more closely resemble the robust zooecia of the living ctenostome *Arachnidium clavatum* or *A. hippothoides* [114] (Plate LV, Figure 7, and Plate LVI, Figure 1, respectively). Without a known fossil record for *Arachnidium* [115], however, it is unlikely that the Tully specimens belong to this genus. In contrast, several species of *Ropalonaria* are known from the Middle Devonian, including *R. tenuis* and *R. medialis* [109]; and *R. lambtonensis* [116], all of which occur in Middle Devonian rocks north of London, Ontario [116], in a northwestern extension of the Appalachian Basin. If the Tully specimens belong to *Ropalonaria*, they may represent a new species because the Tully zooids are much more inflated than was apparently the case for the three Middle Devonian species listed above. More detailed work will be required to elucidate this question, however. The Tully specimens are unlikely to belong to the recently described Lower Devonian *Podoliapora doroshivi* [117] because this new ctenostome species has a preserved anatomy which indicates that the zooecia would have had a more rectilinear shape than the rounded, inflated zooecia of the Tully specimens. In addition, *Podoliapora* has a row of protuberances along the midline of the zooecium which the Tully specimens lack.

The ctenostome genera *Allonema* and *Ascodictyon* contain species with robust vesicles not unlike those that must have held the Tully specimens during life. *Allonema* and *Ascodictyon* also have fine punctae perforating the vesicle walls that mirror the protuberances noted in Figure 13J. According to Ulrich and Bassler [114], each of these genera has at least two species known from the Middle Devonian of the Appalachian Basin: *Allonema fusiforme*, *A. moniliforme* var. *aggregatum*, and *Ascodictyon stellatum*, and *A. floreale*. However, *Allonema* and *Ascodictyon* are unusual bryozoa in the sense that they do not have apertures for the extrusion of lophophore and tentacles. Consequently, their zooids have been regarded as deciduous, i.e., external to the preserved vesicles, and attached to them by means of a thin thread [115]. The Tully specimens, however, have a well-developed collar and lateral stolons, as illustrated in Figure 13. These features are typical of more “normal” ctenostomes, so that we believe that the Tully specimens are unlikely to belong to either *Allonema* or *Ascodictyon*. We also note that Wilson and Palmer [118,119] have forcefully argued that *Allonema* and *Ascodictyon* should be removed from the Bryozoa because their preserved anatomy is so different from that of true Bryozoans. The collar seen in Figure 13H,I indicates that the Tully specimens are bryozoans, and so could not be either *Allonema* or *Ascodictyon*.

Paleozoic ctenostomes, including *Ropalonaria*, are usually preserved as ichnofossils, i.e., as excavations or tunnels made by these encrusters in or on the shell material of larger benthic organisms which they colonize [120]. Alternatively, they are preserved via bioimmuration processes, e.g., by other organisms overgrowing the bryozoans and preserving them as impressions in their hard tissues [121,122]. Among bryozoans, it is ctenostome stolons and vesicles that most often are preserved by these preservational mechanisms. In contrast, the zooecia of Paleozoic ctenostomes are largely unknown. However, as the collars indicate, the specimens illustrated in Figure 13H,I are zooecia. They considerably pre-date the Middle Triassic bioimmured Muschelkalk ctenostome zooecia of Todd and Hagdorn [123], but are slightly younger than zooecia preserved in microcrystalline phosphate of the Lockhovian *Podoliapora doroshivi* from eastern Ukraine recently described by Otempaska [117]. Although zooecia of *P. doroshivi* are currently the oldest known ctenostome zooecia, the Tully zooecia reported here are the oldest ctenostome zooecia known from North America.

### 5.5. *Jinonicellids*

Material: Twenty-six pyritized specimens. Most are incomplete.

Description: The specimens shown in Figure 13K,L are individuals belonging to the species, *Jinonicella kolebabi*. The recurved, hollow tube open at the anterior end and closed at the apical end, and with the snorkel-like secondary tube emanating from the curved part of the main tube is diagnostic for this organism. As indicated in Figure 13 there are two morphs present in the assemblage:

a smooth-surfaced morph (Figure 13L), which is much the more common of the two; and a rare ribbed morph (Figure 13K) in which the anterior portion of the main tube has transverse ribs separated from one another by about 50  $\mu\text{m}$ . The jinonicellid specimen described by Peel and Jepson [124] from the Silurian of Gotland appear to have what these authors interpret as transverse growth lines on the main tube [119] (Figures 1 and 2). Between these growth lines, the main tube is slightly inflated [124] (Figure 1A,B), and in this characteristic resembles the transverse ribs we describe here in the Tully specimen illustrated in Figure 13K. Whether the two Tully morphs represent different sexes, populations, or species, or whether they are the result of differential preservation of otherwise morphologically similar individuals, requires further research.

*Jinonicella* is of uncertain affinity. It has been referred to the archaeogastropods by Pokorný [125], who first described and named *Jinonicella*. Dzik [126] thought that *Jinonicella* is a monoplacophoran, and later suggested that it is derived from helcionelloid molluscs [127]. Peel [128] considered that *Jinonicella* may be a precursor of scaphopods. However, Fryda [129] doubted that *Jinonicella* is a mollusc. Yochelson [130] also questioned whether *Janospira*, an apparently closely allied form, is molluscan.

## 6. Discussion

### 6.1. Algal and Acritarch Taphonomy

Partly or completely pyritized acritarchs and microalgae have been described from sites in northern Europe, eastern North America, central Asia, and Australia, and from rocks of Cryogenian, Ediacaran, Ordovician, Silurian, and Devonian age [6,14–16,18,25,26,56]. However, pyritization as a preservational process for such microfossils is not well understood. Schieber and Baird [16] examined the preservation of pyritized spheroidal tasmanitids from Devonian black shales of the Appalachian and Illinois Basins which resemble our sphaeromorphic forms, as noted above. They envisioned a preservational scenario in which empty algal cysts settled to an anaerobic muddy substrate where they were pyritized and filled with authigenic pyrite framboids which were then diagenetically cemented together with fine grained pyrite cement. In their model, the final form of an individual specimen depended on the relative rates of sedimentation, pyritization, and infilling of the cyst with framboids [16] (Figure 13).

Grey and Willman [57] present a comprehensive study of taphonomic alteration in Neoproterozoic acritarchs from Australia in which they separate taphonomic agents into groups according to the timing of their action in acritarch fossilization and with regard to their effect in modifying original vesicle morphology [57] (Figure 3 and Table 1). In their view also, pyritization is a post-depositional, diagenetic process. They observed that in some cases the occurrence of pyrite framboids within their specimens appeared to be related to the presence of parasitic bacteria infesting the acritarch body. Kaźmierczak and Kremer [26] and Schopf et al. [27] show that subcellular structures within the cell body are sometimes completely or partly pyritized even when the body wall of the organism retains organic compounds or has been silicified. These observations suggest that in some cases the post-mortem development of local concentrations of pyrite within a decaying specimen may not be random or gravitationally controlled, as suggested by Schieber and Baird [16], but rather may reflect subcellular structure of the organism or the pattern of bacterial invasion of the cell. It also suggests that the timing of pyritization in different substructural components of a cell may vary as a function of microenvironmental conditions surrounding and within individual specimens.

As we describe above, a significant proportion of the Tully microfossil assemblage is totally or partly calcified. Thus, it is clear that pyritization cannot be the only taphonomic process operating to preserve the Tully microorganisms; calcification must also be a factor. Kaźmierczak and Kremer [2] (Figures 12 and 13) advance a multi-phase model for the preservation of calcified acritarchs in Late Devonian limestones of Poland that seems applicable to the Tully material. In this model, dead planktonic acritarchs with Ca-enriched, mucilaginous envelopes and studded with tiny calcite crystallites sink quickly post-mortally to the substrate. Calcification continues within the substrate

with the calcifying mucilage becoming the sparry calcite halo surrounding the fossilized cell body. Organic components of the body wall can be retained in the resulting microfossil depending on the extent of post-depositional calcification.

### 6.2. Preservation of the Tully Microflora

Our scenario for the preservation of the Tully algae and acritarchs borrows heavily from the preservation models outlined above. In our view, the idea of dead and dying planktonic cells and evacuated cysts settling through the water column to an essentially anoxic substrate best explains the occurrence of the Tully microfossils. We see the transformation of living algae and acritarchs to mineralized microfossils as the result of the three stage process diagrammed in Figure 14.

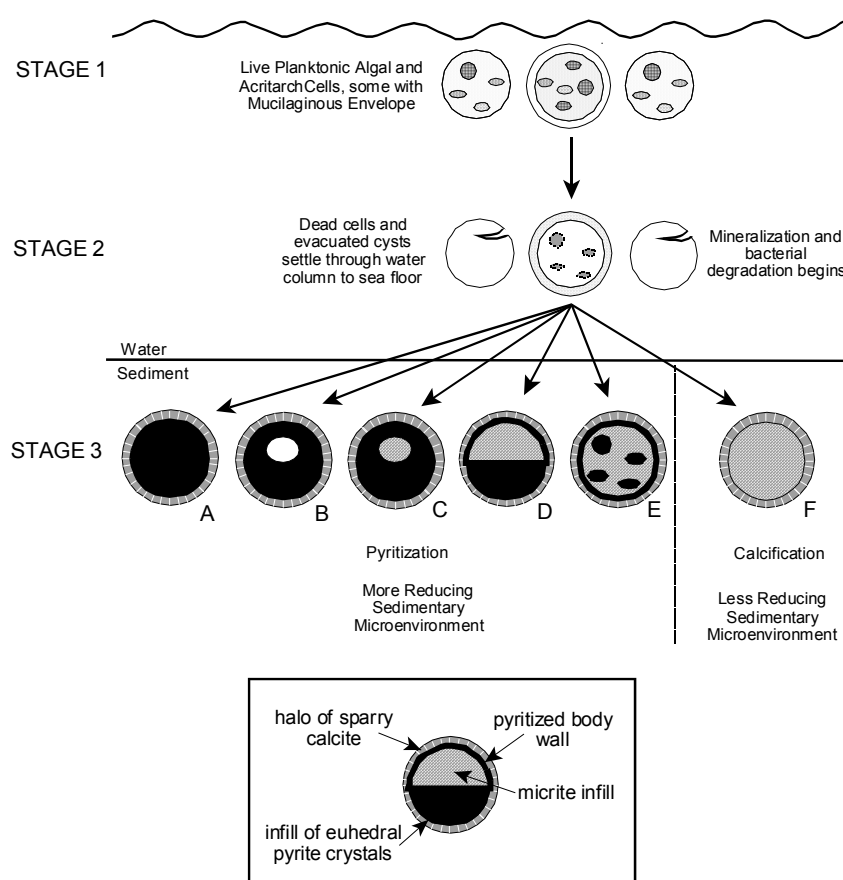


**Figure 14.** Taphonomy of the Tully microflora. Model for the mineralization of algal and acritarch cells preserved in the Lower Tully Limestone at Lock Haven, PA. Arrows indicate passage between preservational stages. They do not indicate that only dead cells rather than cysts give rise to mineralized material in Stage 3. **(STAGE 1)** Live planktonic algal and acritarch cells, some with a mucilaginous envelope, dispersed in the oxygenated surface waters of the Appalachian Seaway; **(STAGE 2)** Settling through the water column of empty cysts and dead cells, and incorporation into the substrate; **(STAGE 3)** Mineralization within the sediment. Formation of halo of sparry calcite crystals, micrite and pyrite infills A–F: different end members of Tully mineralization processes: **(A)** specimen completely pyritized and filled with pyrite; **(B)** pyritized specimen with a hollow interior space; **(C)** pyritized specimen filled primarily with pyrite and a small micrite mass. **(D)** Specimen with pyritized wall and pyrite-micrite infill; **(E)** Specimen with pyritized wall and micrite infill interspersed with globular pyrite clusters; **(F)** Specimen with little or no pyritization and filled entirely with micrite.

Mineralization probably began while Tully specimens were descending toward the seafloor (Stage 2 in our model), and continued after incorporation of the organic remains into the sediment

(Stage 3). In this regard, Kaźmierczak and Kremer [2] present a cogent argument for the initiation of calcification in what we call Stage 2, particularly within the mucilaginous envelope. It is also possible that pyritization began during Stage 2, particularly if a sinking cell or cyst was parasitized by large numbers of reducing bacteria. In such a case, the microenvironment within a bacterial cluster could produce the redox conditions needed for the onset of pyrite formation in the region of the cluster, particularly as the cell settled into more dysoxic waters at depth. Love and Zimmerman [131], Love and Murray [132], Kohn et al. [133], and Folk [134] discuss the active role of bacteria in producing pyrite in oxygen deficient aquatic environments. Maclean et al. [135] illuminate the crucial role played by bacterial biofilms in pyrite framboid formation. In our view, the occurrence of a pyritized frothy layer in some Tully specimens (Figure 11) supports the idea of Stage 2 pyrite formation, as does the occurrence of pyritized surface blisters (Figure 9D) interpreted by Grey and Willman [57] in their Ediacaran acritarchs as due to the activity of invasive bacteria in the early phases of acritarch decomposition. Nevertheless, the folding seen in some Tully specimens (Figure 10), and noted also by Schieber and Baird [16] in their material, undoubtedly is a consequence of sediment dewatering and compaction, as discussed by both Schieber and Baird [16] and Grey and Willman [57], and thus implies that mineralization could not have been far advanced when such specimens reached the sea floor.

Much of the mineralization of Tully specimens would thus appear to have taken place after the decaying cells and cysts reached the substrate but while the substrate was still soft and pliable. The halos of sparry calcite crystals that surround the Tully material (Figures 5A and 6A,C,D) are seen also in the specimens of Kaźmierczak and Kremer [2] (Figures 1–9) and [26] (Figure 2K), and are interpreted by these authors as evidence of calcification continuing within the sediment. In addition, the micritic infill seen in all calcified Tully specimens (Figures 5 and 6A), and in some partly pyritized specimens as well (Figures 6C and 10A), must also be the result of mineralization within the substrate because the primary source of  $\text{Ca}^{2+}$ ,  $\text{CO}_3^{2-}$ , and other ions needed to generate this infill is almost certainly carbonate-rich pore water in the sediment.

Although pyrite may have initially appeared in some specimens as they were sinking downward (Stage 2), most pyritization undoubtedly took place after incorporation of a specimen into the substrate. The degree to which a specimen is pyritized as compared to calcified probably is an expression of the degree of dysoxia and availability of iron and sulfur decomposition products surrounding and within a specimen. The generally darker color of burrow infills and apparent concentration of disseminated pyrite grains within burrows (Figure 4) is an indication of the kind of substrate patchiness that may have occurred in redox conditions, but there is no reason to suspect that other differences, spatially widespread in terms of microfossil dimensions, did not also occur. Preservation in pyrite of body wall (Figure 7D), apparent microbe infestations (Figure 9D), and possible sub-cellular structures (Figure 6B,C) in specimens that are often otherwise primarily calcitic, are all suggestive of the idea that redox potential may have also varied microscopically, i.e., within individual specimens as the breakdown of carbon-rich compounds in these structures induced highly localized conditions of high dysoxia.

### 6.3. Rate of Mineralization

Calcified, and especially pyritized, Tully microfloral specimens preserve many fine details of original structure. This implies that mineralization, both calcification and pyritization, operated rapidly and at a rate sufficient to outpace at least some post-mortem decomposition and decay. The preservation in pyrite of a portion of the mucilaginous envelope (Figure 11) and of possible bacterial concentrations (Figure 9D) is evidence supporting this view. Cysts and body walls are composed of relatively resistant organic compounds, but these compounds are refractory in a relative sense and do not normally long endure post-mortally except in oxygen deficient, fine-grained depositional environments. Thus, preservation of calcified specimens and pyritized specimens retaining their multi-layered body wall (Figures 5B,C and 7D, respectively), also suggests that mineralization was quick-acting in the Tully material. In this context, it is worth noting that pyrite framboids are known

to develop in some modern aquatic depositional systems in time spans of weeks to months [136,137]. Moreover, iron monosulfide pyrite precursors, and pyrite itself, developed within a matter of weeks in the post mortem decomposition experiments described by Allison [138]. Taken together, these observations indicate to us that pyritization of the Tully specimens was accomplished in a very short time frame, and while the substrate in which they were enclosed was still unconsolidated and pliant. Pyritization, and undoubtedly calcification also, was syndepositional.

Although there can be little doubt that Tully pyritization occurred rapidly, there is also evidence that it was a multi-faceted process. Fine-grained pyritic cell walls and mucilage indicate very rapid pyrite development, probably on the scale of weeks or months as suggested above. However, studies done by Rickard et al. [139] and Wilkin and Barnes [140,141] strongly indicate that formation of pyrite crystals equivalent in size (about 10  $\mu\text{m}$ ) to the large, euhedral pyrite crystals filling the interiors of the Tully specimens (Figure 9A–C,E) require considerably more time to develop than fine grained pyrite and small framboids. Thus, the large, euhedral crystals filling specimen interiors were probably more slowly growing than the fine-grained material of the cell walls. Yet, there must have been some degree of contemporaneity in the deposition of these two pyrite morphs because the tears that are visible in the frothy layer covering euhedral crystal arrays (Figure 11B) indicates that there was still some pliability in the pyritizing frothy layer when it encountered the larger, euhedral crystals. This situation can be explained if these larger crystals began infilling the empty cell interiors from the body wall inward. In such a regime, crystals at the inner cell surface and filling excystment scars and splits in the cell wall as in Figure 11B, would be the first to develop and thus could encounter a still flexible frothy layer. Such a crystal growth pattern would also explain specimens with hollow interiors (Figure 9C) or half spheres (Figure 9A) as the result of incomplete inward growth or of interference due to the growth of calcite crystals inside the vesicle. This, in turn implies that calcification and pyritization occurred concurrently. Nevertheless, it is quite clear that calcification is not a prerequisite for simultaneous pyritization of vesicle structures in as much as Winslow [56] found pyritized Tasmanites specimens among her otherwise unmineralized material prepared via the normal process of maceration.

#### 6.4. Depositional Environment of the Microfossil Horizon

The Lower Tully Formation has for many years been viewed as forming on a broad, shallow carbonate platform extending westward into the Appalachian Basin from the Catskill Delta and largely shielded from major siliciclastic sedimentation deriving from Delta runoff by an intervening, east-facing accommodation basin [37,142]. Water depth of this basin was thought to be as little as 20 m in central New York [142] with a gentle downward slope to the southwest [37]. The Tully Formation was seen as consisting of deposits deriving from lagoonal and related shallow platform paleoenvironments [37]. However, microfossil assemblage data from recent work on the organic facies of the Devonian-Mississippian Western Canada Sedimentary Basin [143] indicate that a microfossil assemblage dominated by a small number of planktonic green microalgae, and lacking significant land plant spores is indicative of a deep-water, outer shelf paleoenvironment. This is the composition of the Tully microflora, and therefore implies that the Tully Formation is actually indicative of a deep-water, outer shelf paleoenvironment. In addition, Baird and Brett [38,39], focusing on macrofossils and sedimentary attributes, have also concluded that the Tully Formation is the result of deposition in a deep-water, offshore paleoenvironmental setting. In the Lock Haven area, which is a depocenter for the Lower Tully Formation [37], water depth was probably more than 100 m judging from the data of Stasiuk and Fowler [143].

Baird and Brett [144] have suggested that the Lower Tully beds in this area may be in part turbiditic. Based on their analysis of sedimentary features observed in the Lower Tully beds in the Lock Haven area, and of the paleoecology of the few macrofauna present in these same beds, Baird and Brett [39] also suggest that dysoxic conditions were present in this part of the Appalachian Basin during Lower Tully time. Our discovery of disseminated pyrite grains in the microalgal bed, and the pyritized microbiota itself, are indicative of low oxygen conditions within the sediment, and thus are

consistent with Baird and Brett's [39] interpretation of dysoxia in the basin. They are also consistent with Wignall and Hallam's [145] model of oxygen-restricted biofacies for British black shales, and with Allison et al.'s [146] observation that the presence of tiny pyrite crystals disseminated in Griesbachian micrites is indicative of pyrite in unconsolidated surface sediments and thus of syndepositional substrate anoxia. Compared to the fauna of the Upper Tully Formation at Lock Haven, as detailed by Heckel [36,37], the microfossil horizon preserves an assemblage that is far less species rich than the Upper Tully fauna. Except for the excavators of the burrows that sparsely occur in this unit, the microfossil horizon totally lacks large organisms of any kind. While taphonomic conditions may distort our perception of the assemblage to some extent, it is probably not a significant factor as we have argued above. Thus, the impoverished biota of the microfossil bed, especially the absence of large benthic animals, and the simple substrate ichnology observed in this horizon, place the microfossil bed within Boyer and Droser's [147] most extreme zone of dysoxia for Givetian black shales of western New York. It would appear, therefore, that this zone of dysoxia in New York extended southward into Pennsylvania at least as far as the Lock Haven area. The idea that the overlying water column was oxygenated to some extent during deposition of the microfossil bed is supported by the presence of the microorganisms as well as by the burrows which occur in this horizon.

#### 6.5. Paleoecology of the Tully Microbiota

The arguments we present above indicate that the microfossil horizon at Lock Haven is best viewed as representing offshore, deep water conditions characterized by an essentially anoxic substrate but with sufficient oxygen in the overlying water column to support nektonic and planktonic organisms. This suggests to us that the Lock Haven microbiota consists primarily of organisms living within the water column which were preserved in the microfossil bed when their remains settled to the substrate post-mortally, or when live microorganisms were carried onto the substrate and asphyxiated. This would readily account for the planktonic dacroconarids, ostracods, algae, and acritarchs. The occurrence of the benthic bivalves and gastropods is probably the result of failed recruitment of neonatal individuals. We suggest that these animals were in the process of transforming from their planktonic larval stage and had just begun to secrete shell material when they settled to the sea floor and succumbed to the dysoxia into which they had the misfortune to fall. Mapes and Nützel [148] report a similar example from the Carboniferous Ruddle Shale of Arkansas. As adults most nautiloids were probably nektonic or nektobenthic and would be removed from sediment dysoxia. But the specimen described here is a protoconch, as noted above, and thus represents an animal that had only just hatched. The eggs of modern *Nautilus* are attached to the substrate for lengthy intervals [149,150]. If the reproductive strategy of the Devonian precursors of *Nautilus* was similar, the occurrence of hatchling Tully longicones would seem to require some irregularities in seafloor topography or in the distribution of sediment dysoxia which would allow the eggs to develop above the dysoxic zone, or in a patch of better oxygenated sediment. The preserved hatchlings would represent animals that had the misfortune to swim into the dysoxic zone, or to be carried downwards rather than upwards after emerging from their eggs. The bryozoans may have been epizoans living attached to floating objects or to animals higher up in the water column, or they could have lived in ramose colonies attached to the substrate that were just tall enough to carry them far enough into the water column to acquire the oxygen they needed.

Although the taxonomic status of *Jinonicella* is uncertain, all of the groups to which it has been attributed have benthic lifestyles. The association of this organism with sediment dysoxia is thus an interesting anomaly because it is not what one would expect for a member of the benthos. This association could be explained in terms of a patchy distribution of sediment dysoxia. In this case, the pyritized specimens reported here would represent animals, normally confined to oxygenated patches, that actively or passively travelled to the dysoxic sediment in which we find them. Alternatively, *Jinonicella*, if benthic as an adult, may have had a planktotrophic larval stage, and like the Tully gastropods and bivalves preserved with it, succumbed when the metamorphosing larvae settled

into the dysoxic zone at the sediment-water interface. This seems unlikely for *Jinonicella*, however, because larvae usually grow into adults that are considerably larger than the larvae. All known *Jinonicella* occurrences are of specimens having a maximum size equivalent to specimens described here [125,127,129]. This indicates to us that our specimens are probably not hatchlings. Perhaps the pyritized specimens of *Jinonicella* are telling us that the living organism was planktonic. If so, it probably means that *Jinonicella* does not belong to any of the groups to which it has been referred.

## 7. Conclusions

The lower member of the Givetian Tully Formation of north-central Pennsylvania, USA, contains a mineralized microbiota dominated by microalgae (*Tasmanites*) and acritarchs (*Solisphaeridium?*) Other palynomorphs (e.g., plant spores, scolecodonts, chitinozoans) have not been found. However, the microbiota also contains a variety of millimeter-sized animals including molluscs (nuculoid bivalves, a longiconic cephalopod, and gastropods), ostracodes, ctenostome bryozoans, and animals of uncertain affinity (dacryconarids and jinonicellids). The bryozoans are preserved as zooecia and are the oldest known ctenostome zooecia from North America. Macrofossils do not co-occur with the microfossils, although small burrows are present.

The assemblage is preserved via a complex process of mineralization of organic and crystalline components of the living organisms. Acritarchs and algae are pyritized or calcified, and in some cases are composed of both pyrite and calcite. Preservation of subcellular structures, mucilaginous envelopes, and bacterial infestations indicates that mineralization was fast-acting, bacterially mediated, and probably began while dead cells and empty vesicles settled through the water column immediately after death. Creased and folded specimens indicate that many individuals were still soft and pliable when first incorporated into the sediment, and that mineralization was a syndepositional process. Animals with carbonate skeletons (e.g., molluscs) are commonly found as pyritized steinkerns.

The substrate in which these microorganisms came to rest contained disseminated pyrite and was strongly dysoxic, although sediment dysoxia appears to have varied somewhat in intensity from place to place, e.g., greater within burrows than outside them. However, the overlying water column was oxygenated as attested by the presence of the microorganisms and the burrows. The low species richness of the microflora and the absence of terrestrially derived microfloral elements suggests that the microfossil horizon was deposited in an offshore, deep water setting. This interpretation is consistent with recent views on the depositional environment of the Lock Haven Tully Formation [38,39] based on sedimentological and macrofossil considerations.

The algae and acritarchs were planktonic, but there is no evidence that their abundance varied seasonally, or that their deposition was seasonally induced. Among the microfauna, the dacryconarids and probably the ostracodes were also planktonic. Jinonicellids have been referred to a variety of benthic groups, but a benthic life habit in Tully sediment for these enigmatic forms seems unlikely given the dysoxic sedimentary environment. We suggest that they were actually planktonic, and probably not members of any of the groups to which they have been linked. The bivalves and gastropods preserved in the microfossil horizon are best interpreted as planktotrophic larvae that had just begun their metamorphosis to shell secreting juveniles and were asphyxiated when they settled onto the dysoxic substrate surface. The pyritized cephalopod shell in our assemblage is a protoconch and may represent a newly hatched animal that was, upon hatching or soon after, caught in the low oxygen environment at the substrate surface. The bryozoans were probably attached to objects or organisms floating or swimming in the water column well above the dysoxic environment in the substrate.

**Acknowledgments:** We are grateful to former student Michelle T.W. Carter, for her assistance in the early phases of this work, particularly with specimen collection and preparation. We also appreciate the guidance of Gordon C. Baird, State University of New York-Fredonia, in helping us understand the biostratigraphy of the Tully Formation; Roger Cuffey, Pennsylvania State University, for his advice on bryozoans; Józef Kaźmierczak and Barbara Kremer, Polish Academy of Sciences, for their encouragement during the early preparation of this paper; Richard H. Lindeman, Skidmore College, for his help in identifying the dacryconarids and in measuring the Tully exposure with us in 2014; and E. Reed Wicander, Central Michigan University, for advising us on algal and

acritarch taxonomy. The presentation of this research was greatly assisted by three anonymous reviewers for this journal. We are grateful to all of these individuals for their contributions. Errors occurring in these pages are due solely to us, not to them. William J. L'Amoreux, College of Staten Island, assisted with the SEM study. This work was supported by Professional Staff Congress—City University of New York research awards to J.A.C. and R.B.C.

**Author Contributions:** J.A.C., R.B.C. and J.O.B. collected and examined specimens and analyzed the data. J.A.C. and R.B.C. wrote the paper.

**Conflicts of Interest:** The authors declare no conflict of interest. The funding sponsors had no role in the design of the study; in the collection, analyses, or interpretation of data; in the writing of the manuscript, and in the decision to publish the results.

## References

- Williamson, W.C. On the organisation of the fossil plants of the Coal-Measures, Part X. Including an examination of the supposed radiolarians of the Carboniferous rocks. *Philos. Trans. R. Soc. Lond. Ser. B* **1881**, *148*, 9–43.
- Kaźmierczak, J.; Kremer, B. Early post-mortem calcified Devonian acritarchs as a source of calcispheric structures. *Facies* **2005**, *51*, 573–584. [[CrossRef](#)]
- Thomas, H.D. Origin of spheres in the Georgetown Limestone. *J. Paleontol.* **1932**, *6*, 100–101.
- Stanton, R.J., Jr. Radiosphaerid calcispheres in North America and remarks on calcisphere classification. *Micropaleontology* **1967**, *13*, 465–472. [[CrossRef](#)]
- Masters, B.A.; Scot, R.W. Calcispheres and nannoconids. In *The Encyclopedia of Paleontology*; Fairbridge, R.W., Jablonski, D., Eds.; Dowden, Hutchinson and Ross: Stroudsburg, PA, USA, 1979; pp. 167–170.
- Wanner, J. Gesteinsbildende Foraminiferen aus Malm und Unterkreide des östlichen Ostendischen Archipels. *Paläontol. Zeits* **1940**, *22*, 75–99.
- Kettenbrink, E.C., Jr.; Toomey, D.F. Distribution and paleoecological implication of calcareous Foraminifera in the Devonian Cedar Valley Formation of Iowa. *J. Foraminifer. Res.* **1975**, *5*, 176–187. [[CrossRef](#)]
- Cayuex, L. Les Calcisphères typiques sont des Algues siphonnées. *C. R. Acad. Sci. Paris* **1929**, *188*, 594–597.
- Lombard, A.; Monteyne, R. Calcisphères dans le Frasnien de Bois-de-Villiers (Namur). *Bull. Soc. Belg. Géol. Paléont. Hydrol.* **1952**, *61*, 13–25.
- Aldridge, R.J.; Armstrong, H. Spherical phosphatic microfossils from the Silurian of North Greenland. *Nature* **1981**, *292*, 531–533. [[CrossRef](#)]
- Holmer, L.E. Ordovician mazuelloids and other microfossils from Västergötland. *Geologiska Föreningen i Stockholm Förhandlingar* **1986**, *109*, 66–71. [[CrossRef](#)]
- Kozur, H.W. Muellersphaerida, eine neue Ordnung von Mikrofossilien unbekannter systematischer Stellung aus dem Silur und Unterdevon von Ungarn. *Geol. Paläontol. Mittlungen Innsbruck* **1984**, *13*, 125–148.
- Porebska, E.; Koszłowska, E. Mazzuelloids—Apatite algae from the Lower Paleozoic of the Bardzkie Mountains (Sudety Mountains, SW Poland). *Przegląd Geologiczny* **2001**, *49*, 1050–1060.
- Loydell, D.K.; McMillan, I.; Barron, H.F. Muellersphaerids from the Llandovery of western mid-Wales. *J. Micropaleontol.* **1988**, *7*, 243–246. [[CrossRef](#)]
- Tibbs, S.L.; Briggs, D.E. G.; Prössl, K. Pyritisation of plant microfossils from the Devonian Hunsrück Slate of Germany. *Palaöntol. Z.* **2003**, *77*, 241–246. [[CrossRef](#)]
- Schieber, J.E.; Baird, G. On the origin and significance of pyrite spheres in Devonian black shales of North America. *J. Sediment. Res.* **2001**, *71*, 155–166. [[CrossRef](#)]
- Kaźmierczak, J.; Ittekkot, V.; Degens, E.T. Biocalcification through time environmental challenge and cellular response. *Paläontol. Z.* **1985**, *59*, 15–33. [[CrossRef](#)]
- Kremer, B. Mazuelloids: Products of post-mortem phosphatization of acanthomorphic acritarchs. *Palaios* **2005**, *20*, 27–36. [[CrossRef](#)]
- Evitt, W.R. A discussion and proposals concerning fossil dinoflagellates, hytrichospheres, and acritarchs, I. *Proc. Natl. Acad. Sci. USA* **1963**, *48*, 158–164. [[CrossRef](#)]
- Evitt, W.R. A discussion and proposals concerning fossil dinoflagellates, hytrichospheres, and acritarchs, II. *Proc. Natl. Acad. Sci. USA* **1963**, *48*, 298–302. [[CrossRef](#)]
- Martin, F. Acritarchs: A review. *Biol. Rev.* **1993**, *68*, 475–538. [[CrossRef](#)]
- Colbath, G.K.; Grenfell, H.R. Review of biological affinities of Paleozoic acid-resistant, organic-walled eukaryotic algal microfossils (including acritarchs). *Rev. Palaeobot. Palynol.* **1995**, *86*, 287–314. [[CrossRef](#)]

23. Kempe, A.; Schopf, J.W.; Altermann, W.; Kudryavtsev, A.B.; Heckl, W.M. Atomic force microscopy of Precambrian microscopic fossils. *Proc. Natl. Acad. Sci. USA* **2002**, *99*, 917–920. [[CrossRef](#)] [[PubMed](#)]
24. Kempe, A.; Wirth, A.; Altermann, W.; Stark, R.W.; Schopf, J.W.; Heckl, W.M. Focused ion beam preparation: An in situ nanoscopic study of Precambrian acritarchs. *Precamb. Res.* **2005**, *140*, 36–54. [[CrossRef](#)]
25. Marshall, C.P.; Javaux, E.J.; Knoll, A.H.; Walter, M.R. Combined micro-Fourier transform infrared (FTIR) spectroscopy and micro-Raman spectroscopy of Precambrian acritarchs: A new approach to paleobiology. *Precamb. Res.* **2005**, *138*, 208–224. [[CrossRef](#)]
26. Kaźmierczak, J.; Kremer, B. Spore-like bodies in some early Paleozoic acritarchs: Clues to chlorococcalean affinities. *Acta Palaeontol. Pol.* **2009**, *54*, 541–551. [[CrossRef](#)]
27. Schopf, J.W.; Kudryavtsev, A.B.; Sergeev, V.N. Confocal laser scanning microscopy and Raman imagery of the Late Neoproterozoic Chichkan microbiota of south Kazakhstan. *J. Paleontol.* **2010**, *84*, 402–416. [[CrossRef](#)]
28. Moczydłowska, M.; Landing, E.; Zang, W. Palacios, T. Proterozoic plankton and timing of Chlorophyte origins. *Palaeontology* **2011**, *54*, 721–734. [[CrossRef](#)]
29. Cohen, P.; Knoll, A.; Kodner, R. Large spinose microfossils in Ediacaran rocks as resting stages of early animals. *Proc. Nat. Acad. Sci. USA* **2009**, *106*, 6519–6524. [[CrossRef](#)] [[PubMed](#)]
30. Cohen, P.; Kelly, A.; Kodner, R. Taxonomic affinity of Late Devonian organic-walled microfossils: Interpretations and implications. *Geol. Soc. Am. Abstr. Annu. Meet.* **2016**, *48*. [[CrossRef](#)]
31. Grabau, A.W. Stratigraphic relationships of the Tully limestone and the Genesee shale in eastern North America. *Geol. Soc. Am. Bull.* **1917**, *28*, 945–958.
32. Trainer, D.W., Jr. The Tully Limestone of central New York. *N. Y. State Mus. Bull.* **1932**, *291*, 1–43.
33. Willard, B. Hamilton Group of central Pennsylvania. *Geol. Soc. Am. Bull.* **1935**, *46*, 195–224. [[CrossRef](#)]
34. Willard, B. Middle and Upper Devonian. In *The Devonian of Pennsylvania: Pennsylvania Geol. Survey; 4th Series; General Geol. Rp.t G19*; Willard, B., Swartz, F.M., Cleaves, A.B., Eds.; Pennsylvania Geological Survey: Harrisburg, PA, USA, 1939; pp. 131–308.
35. Johnson, K.G.; Friedman, G.M. The Tully clastic correlative (upper Devonian) of New York State: A model for recognition of alluvial, dune (?), tidal, nearshore (bar and lagoon), and offshore sedimentary environments in a tectonic delta complex. *J. Sediment. Res.* **1969**, *39*, 452–485.
36. Heckel, P.H. Devonian Tully Limestone in Pennsylvanian and comparison of type Tully Limestone of New York. *Pa. Geol. Surv. Bull. 4th Ser.* **1969**, *IC60*, 1–33.
37. Heckel, P.H. *Nature, Origin, and Significance of the Tully Limestone*; Geological Society of America Special Paper 138; Geological Society of America: Boulder, CO, USA, 1973; p. 244.
38. Baird, G.C.; Brett, C.E. Shelf and off-shelf deposits of the Tully Formation in New York and Pennsylvania: Faunal incursions, eustacy, and tectonics. *Courier-Forschungsinstitut Senckenberg* **2003**, *242*, 141–156.
39. Baird, G.C.; Brett, C.E. Late Givetian Taghanic bioevents in New York State: New discoveries and questions. *Bull. Geosci.* **2008**, *83*, 357–370. [[CrossRef](#)]
40. Kirchgasser, W.T.; Baird, G.C.; Brett, C.E. Regional placement of the Middle/Upper Devonian (Givetian-Frasnian) boundary in western New York State. In *Devonian of the World; Memoir 14, Part 2*; McMillan, N.J., Embry, A.F., Glass, D.J., Eds.; Canadian Society of Petroleum Geologists: Calgary, AB, Canada, 1988; pp. 113–118.
41. Brett, C.E.; Baird, G.C. B-5 depositional sequences, cycles, and foreland basin dynamics in the late Middle Devonian (Givetian) of the Genesee Valley and western Finger Lakes region. In *Field Trip Guidebook for New York State Geological Association 66th Annual Meeting*; Brett, C.E., Scatterday, J., Eds.; New York State Geological Association: Albany, NY, USA, 1994; pp. 505–586.
42. Weary, D.J.; Harris, A.G. Early Frasnian (Late Devonian) conodonts from the Harrell Shale, western foreland fold-and-thrust belt, West Virginia, Maryland, and Pennsylvania Appalachians, U.S.A. *Cour. Forsch. Inst. Senckenburg* **1994**, *168*, 195–225.
43. Brown, J.O. Biostratigraphy and Paleocology of the Givetian Hamilton Group in Pennsylvania and New York. Ph.D. Thesis, City University of New York, New York, NY, USA, 2001.
44. Zambito, J.J., IV; Brett, C.E.; Baird, G.C. The Late Middle Devonian (Givetian) Global Taghanic biocrisis in its type area (Northern Appalachian Basin): Geologically rapid faunal transitions driven by global and local environmental changes. In *Earth and Life: International Year of Planet Earth*; Talent, J., Ed.; Springer Science + Business Media B.V.: Dordrecht, The Netherlands, 2012; pp. 677–702.

45. Johnson, J.G. Taghanic onlap and the end of North American Devonian provinciality. *Geol. Soc. Am. Bull.* **1970**, *81*, 2077–2105. [[CrossRef](#)]
46. Brett, C.E.; Baird, G.C.; Bartholomew, A.J. Biofacies recurrence in the Middle Devonian of New York State: An example with implications for evolutionary paleoecology. *Palaios* **2007**, *22*, 306–324. [[CrossRef](#)]
47. Day, J. Faunal signatures of Middle-Upper Devonian depositional sequences and sea-level fluctuations in the Iowa Basin. In *Paleozoic Sequence Stratigraphy: Views from the North American Craton*; Geological Society of America Special Paper 306; Witzke, B.J., Ludvigson, G.A., Day, J., Eds.; Geological Society of America: Boulder, CO, USA, 1996; pp. 277–300.
48. House, M.R. Strength, timing, setting and cause of the mid-Paleozoic extinctions. *Palaeogeogr. Palaeoclimatol. Palaeoecol.* **2002**, *181*, 5–25. [[CrossRef](#)]
49. Aboussalam, S.Z. Das “Taghanic-Event” in höheren Mittel-Devonien von West-Europa und Marokko. *Münstersche Forsch. Geol. Paläontol.* **2003**, *97*, 1–322.
50. Aboussalam, S.Z.; Becker, R.T. The global Taghanic Biocrisis (Givetian) in the eastern Anti-Atlas, Morocco. *Palaeogeogr. Palaeoclimatol. Palaeoecol.* **2011**, *304*, 136–164. [[CrossRef](#)]
51. Harris, A.G.; Sweet, W.C. Mechanical and chemical techniques for separating microfossils from rock, sediment, and residue matrix. In *Paleotechniques*; Paleontological Society Special Paper 4; Feldman, R.M., Chapman, R.E., Hannibal, J.T., Eds.; The Paleontological Society: Boulder, CO, USA, 1989; pp. 70–86.
52. Maples, C.G.; Waters, J.A. Use of drain cleaner in processing shale samples. *J. Paleontol.* **1990**, *64*, 484–485. [[CrossRef](#)]
53. Pojeta, J., Jr.; Balanc, M. Heating and quenching of fossils. In *Paleotechniques*; Paleontological Society Special Paper 4; Feldman, R.M., Chapman, R.E., Hannibal, J.T., Eds.; The Paleontological Society: Boulder, CO, USA, 1989; pp. 218–222.
54. Krukowski, S.T. Sodium metatungstate: A new heavy-mineral separation medium for the extraction of conodonts from insoluble residues. *J. Paleontol.* **1988**, *62*, 314–316. [[CrossRef](#)]
55. Schieber, J. The role of an organic slime matrix in the formation of pyritized burrow trails and pyrite concretions. *Palaios* **2002**, *17*, 104–109. [[CrossRef](#)]
56. Winslow, M.R. *Plant Spores and Other Microfossils from Upper Devonian and Lower Mississippian Rocks of Ohio*; United States Geological Survey Professional Paper 364; United States Geological Survey: Reston, VA, USA, 1962; p. 90.
57. Grey, K.; Willman, S. Taphonomy of Ediacaran acritarchs from Australia: Significance for taxonomy and biostratigraphy. *Palaios* **2009**, *24*, 239–256. [[CrossRef](#)]
58. Burden, E.T.; Quinn, L.; Nowlan, G.S.; Bailey-Nill, L.A. Palynology and micropaleontology of the Clam Bank Formation (Lower Devonian of western Newfoundland, Canada). *Palynology* **2002**, *26*, 185–215. [[CrossRef](#)]
59. Colbath, G.K. Fossil prasinophycean phycmata (Chlorophyta) from the Silurian Bainbridge Formation, Silurian, USA. *Phycologia* **1983**, *22*, 249–265. [[CrossRef](#)]
60. Filipiak, P. Late Devonian and Early Carboniferous acritarchs and prasinophytes from the Holy Cross Mountains (central Poland). *Rev. Paleobot. Palynol.* **2005**, *134*, 1–26. [[CrossRef](#)]
61. Agić, H.; Moczydłowska, M.; Yin, L.-M. Affinity, life cycle, and intracellular complexity of organic-walled microfossils from the Mesoproterozoic of Shanxi, China. *J. Paleontol.* **2015**, *89*, 28–50. [[CrossRef](#)]
62. Strother, P.K. Acritarchs. In *Palynology: Principles and Applications*; Jansonius, J., McGregor, D.C., Eds.; American Association of Stratigraphic Palynologists Foundation: Dallas, TX, USA, 1996; Volume 1, pp. 81–106.
63. Filipiak, P. Lower Famennian phytoplankton from the Holy Cross Mountains, Central Poland. *Rev. Paleobot. Palynol.* **2009**, *157*, 326–338. [[CrossRef](#)]
64. Ghavidel-Syooki, M.; Hassanzadeh, J.; Vecoli, M. Palynology and isotope geochronology of the Upper Ordovician–Silurian successions (Ghelli and Soltan Maidan Formations) in the Khoshyeilagh area, eastern Alborz Range, northern Iran; stratigraphic and palaeogeographic implications. *Rev. Paleobot. Palynol.* **2011**, *164*, 251–271. [[CrossRef](#)]
65. Miller, M.A.; Williams, G.L. *Velatasphaera hudsonii* gen. et sp. nov., an Ordovician acritarch from Hudson Strait, North West Territories, Canada. *Palynology* **1988**, *12*, 121–127. [[CrossRef](#)]
66. Fritsch, F.E. *The Structure and Reproduction of the Algae*; Cambridge University Press: Cambridge, UK, 1965; p. 791.
67. Boney, A.D. Mucilage: The ubiquitous algal attribute. *Br. Phycol. J.* **1981**, *16*, 115–132. [[CrossRef](#)]

68. Oertel, A.; Aichinger, N.; Hochrieter, R.; Thalhamer, J.; Ursula Lütz, U. Analysis of mucilage secretion and excretion in *Micrasterias* (Chlorophyta) by means of immunoelectron microscopy and digital time lapse video microscopy. *J. Phycol.* **2004**, *40*, 711–720. [[CrossRef](#)]
69. Kreinitz, L.; Hegewald, E.H.; Hepperle, D.; Huss, V.A.R.; Rohr, T.; Wolf, F. Phylogenetic relationships of *Chlorella* and *Parachlorella* gen. nov. (Chlorophyta, Trebouxiophyceae). *Phycologia* **2004**, *43*, 529–542. [[CrossRef](#)]
70. Moldowan, J.M.; Talyzina, N.M. Biogeochemical evidences for dinoflagellate ancestors in the early Cambrian. *Science* **1998**, *281*, 1168–1170. [[CrossRef](#)] [[PubMed](#)]
71. Arouri, K.; Greenwood, P.F.; Walter, M.R. A possible chlorophyceae affinity of some Neoproterozoic acritarchs. *Org. Geochem.* **1999**, *30*, 1323–1337. [[CrossRef](#)]
72. Javaux, E.J.; Marshall, C.P. A new approach in deciphering early protist paleobiology and evolution: Combined microscopy and microchemistry of single Proterozoic acritarchs. *Rev. Paleobot. Palynol.* **2006**, *139*, 1–15. [[CrossRef](#)]
73. Kodner, R.B.; Pearson, A.; Summons, R.E.; Knoll, A.H. Sterols in red and green algae: Quantification, phylogeny, and relevance for the interpretation of geologic steranes. *Geobiology* **2008**, *6*, 411–420. [[CrossRef](#)] [[PubMed](#)]
74. Moczydłowska, M. Life cycle of early Cambrian microalgae from the *Skiagia*-plexus acritarchs. *J. Paleontol.* **2010**, *84*, 216–230. [[CrossRef](#)]
75. Lewis, L.A.; McCourt, R. Green algae and the origin of land plants. *Am. J. Bot.* **2004**, *91*, 1535–1556. [[CrossRef](#)] [[PubMed](#)]
76. Adl, S.M.; Alastair, G.B.; Simpson, M.A.; Farmer, R.A.; Andersen, O.R.; Barta, J.R.; Bowser, S.S.; Brugerolle, G.; Fensome, R.A.; Fredericq, S.; et al. The New Higher Level Classification of Eukaryotes with Emphasis on the Taxonomy of Protists. *J. Eukaryot. Biol.* **2005**, *52*, 399–451. [[CrossRef](#)] [[PubMed](#)]
77. Rodriguez-Ezpeleta, N.; Brinkmann, H.N.; Burger, G.; Roger, A.J.; Gray, M.W.; Herve, P.; Lan, B.F. Toward resolving the eukaryotic tree: The phylogenetic positions of jakobids and cercozoans. *Curr. Biol.* **2005**, *17*, 1420–1425. [[CrossRef](#)] [[PubMed](#)]
78. O’Kelly, C.J. The origin and early evolution of green plants. In *Evolution of Primary Producers in the Sea*; Falkowski, P.G., Knoll, A.H., Eds.; Academic Press Elsevier: Amsterdam, The Netherlands, 2007; pp. 287–309.
79. Termel, M.; Brouard, J.-S.; Gagnon, C.; Otis, C.; Lemieux, C. Deep division in the Chlorophyceae (Chlorophyta) revealed by Chloroplast phylogenomic analyses. *J. Phycol.* **2008**, *44*, 739–750. [[CrossRef](#)] [[PubMed](#)]
80. Wicander, E.R.; Schopf, J.W. Microorganisms from the Kalkberg Limestone (Lower Devonian) of New York State. *J. Paleontol.* **1974**, *48*, 74–77.
81. Wood, G.D.; Clendening, J.A. Organic-Walled Microphytoplankton and Chitinozoans from the Middle Devonian (Givetian) Boyle Dolomite of Kentucky, U.S.A. *Palynology* **1985**, *9*, 133–145. [[CrossRef](#)]
82. Knoll, A.H.; Golubic, S. Anatomy and taphonomy of a Precambrian algal stromatolite. *Precamb. Res.* **1979**, *10*, 115–151. [[CrossRef](#)]
83. Cavalier-Smith, T. A revised six-kingdom system of life. *Biol. Rev.* **1998**, *73*, 203–266. [[CrossRef](#)] [[PubMed](#)]
84. Tappan, H. *The Paleobiology of Plant Protists*; W.H. Freeman & Co.: San Francisco, CA, USA, 1980; p. 1028.
85. Newton, E.T. On “tasmanite” and Australian “white coal”. *Geol. Mag. Ser. 2* **1875**, *12*, 337–342. [[CrossRef](#)]
86. Schopf, J.M.; Wilson, L.R.; Bentall, R. *An Annotated Synopsis of Paleozoic Fossil Spores and the Definition of Generic Groups*; Illinois State Geological Survey, Report of Investigations 91; State of Illinois, Division of the Geological Survey: Urbana, IL, USA, 1944; p. 74.
87. Knoll, A.H.; Swett, K. Micropalaeontology of the Late Proterozoic Veteranen Group, Spitsbergen. *Palaeontology* **1985**, *28*, 451–473.
88. Samuelsson, J.; Dawes, P.R.; Vidal, G. Organic-walled microfossils from the Proterozoic Thule Supergroup, Northwest Greenland. *Precamb. Res.* **1999**, *96*, 1–23. [[CrossRef](#)]
89. Boalch, G.T.; Guy-Ohlson, G. *Tasmanites*, the correct name for *Pachysphaera* (Prasinophyceae, Pterospmataceae). *Taxonomy* **1992**, *41*, 529–531. [[CrossRef](#)]
90. Fensome, R.A.; Williams, G.L.; Barss, M.S.; Freeman, J.M.; Hill, J.M. *Acritarchs and Fossil Prasinophytes: An Index to Genera, Species, and Intraspecific Taxa*; American Association of Stratigraphic Palynologists Foundation Contributions Series No. 25; American Association of Stratigraphic Palynologists Foundation: Houston, TX, USA, 1990; p. 771.

91. Mullins, G.L.; Aldridge, R.J.; Dorning, K.J.; LeE Herisse, A.; Jun, L.; Moczydłowska-Vidal, M.; Molyneux, S.G.; Servais, T.; Wicander, R. The PhytoPal Taxonomic Database (Taxon List). 2007. Available online: [www.le.ac.uk/geology/glm2/phytopal/taxa.pdf](http://www.le.ac.uk/geology/glm2/phytopal/taxa.pdf) (accessed on 27 December 2014).
92. Wicander, E.R. *A Catalog and Biostratigraphic Distribution of North American Devonian Acritarchs*; American Association of Stratigraphic Palynologists Foundation Contributions Series No. 10; American Association of Stratigraphic Palynologists Foundation: Houston, TX, USA, 1983; p. 133.
93. Downie, C.; Evitt, W.R.; Sarjeant, W.A.S. Dinoflagellates, hystrichospheres and the classification of the acritarchs. *Stanf. Univ. Publ. Geol. Sci.* **1963**, *7*, 1–16.
94. Staplin, F.L.; Jansonius, J.; Pocock, S.A.J. Evaluation of some acritarchous hystrichosphere genera. *Neues Jahrb. Geol. Paläontol. Abhand.* **1965**, *123*, 167–201.
95. Sarjeant, W.A.S. Microplankton from the Upper Callovian and Lower Oxfordian of Normandy. *Rev. Micropaleontol.* **1968**, *10*, 221–242.
96. Moczydłowska, M. Cambrian acritarchs from Upper Silesia, Poland—biochronology and tectonic implications. *Foss. Strat.* **1998**, *46*, 1–121.
97. Deflandre, G. Microplancton des mers jurassiques conservé dans les marnes de Villers-sur-Mer (Calvados). Étude liminaire et considérations générales. *Travaux Station Zoologique Wimereux* **1938**, *13*, 147–200.
98. Moczydłowska, M. Acritarch biostratigraphy of the Lower Cambrian and the Precambrian–Cambrian boundary in southeastern Poland. *Foss. Strat.* **1991**, *29*, 1–127.
99. Moczydłowska, M.; Stockfors, M. Acritarchs from the Cambrian–Ordovician Boundary Interval on Kolguev Island, Arctic Russia. *Palynology* **2004**, *28*, 15–73. [[CrossRef](#)]
100. Heisecke, A.M. Microplancton de la Formación Roca de la Provincia de Neuquén. *Ameghiniana* **1970**, *7*, 225–263.
101. Wicander, E.R. Upper Devonian–Lower Mississippian acritarchs and prasinophycean algae from Ohio, U.S.A. *Palaeontogr. Abt. B* **1974**, *148*, 9–43.
102. Wicander, E.R.; Playford, G. Acritarchs and Spores from the Upper Devonian Lime Creek Formation, Iowa, U.S.A. *Micropaleontology* **1985**, *31*, 97–138. [[CrossRef](#)]
103. Wicander, R.; Wood, G.D. The use of microplankton and chinozoa for interpreting transgressive/regressive cycles in the Rapid Member of the Cedar Valley Formation (Middle Devonian) Iowa. *Rev. Palaeobot. Palynol.* **1997**, *98*, 125–152. [[CrossRef](#)]
104. Smelror, M.; Leereveld, H. Dinoflagellate and acritarch assemblages from the Late Bathonian to Early Oxfordian of Montagne Crussol, Rhône Valley, Southern France. *Palynology* **1989**, *13*, 121–141. [[CrossRef](#)]
105. Brown, J.O.; Chamberlain, J.A., Jr.; Perlmutter, B. A pyritic micro-molluscan fauna at the base of the Lower Tully Formation (upper Givetian) from Lock Haven, Pennsylvania. *Geol. Soc. Am. Abstr. Program Annu. Meet.* **1998**, *30*, A-34.
106. Chamberlain, J.A., Jr.; Brown, J.O. First occurrence of the enigmatic microfossil *Jinonicella* in North America: Tully Limestone (Givetian) of central Pennsylvania. *Geol. Soc. Am. Abstr. Program Annu. Meet.* **2000**, *32*, A-10.
107. Bailey, J.B. Systematics, Hinge, and Internal Morphology of the Devonian Bivalve, *Nuculoidea corbuliformis* (Hall and Whitfield). *J. Paleontol.* **1986**, *60*, 1177–1185. [[CrossRef](#)]
108. Linsley, D.M. *Devonian Paleontology of New York*; Special Publication 21; Paleontological Research Institution: Ithaca, NY, USA, 1994; p. 472.
109. Brett, C.E.; Cottrell, J.F. Substrate specificity in the Devonian tabulate coral *Pleurodictyum*. *Lethaia* **1982**, *15*, 247–262. [[CrossRef](#)]
110. Flower, R.H. Classification of Devonian Nautiloids. *Am. Midl. Nat.* **1945**, *33*, 675–724. [[CrossRef](#)]
111. Tillman, J.R. Ostracodes of the Superfamilies Beyrichiacea and Drepanellacea from Middle Devonian Rocks of Central Ohio. *J. Paleontol.* **1984**, *58*, 234–253.
112. Lindemann, R.H.; Yochelson, E.L. *Viriatellina* (Dacryoconarida) from the Middle Devonian Ludlowville Formation at Alden, New York. *J. Paleontol.* **1992**, *66*, 93–199. [[CrossRef](#)]
113. Lindemann, R.H.; Skidmore College, Saratoga Springs, NY, USA. Personal communication, 2014.
114. Ulrich, E.O.; Bassler, R.S. A revision of the Paleozoic Bryozoa, Part 1. On genera and species of Ctenostomata. *Smithson. Misc. Collect. Q. Issue* **1904**, *2*, 256–298.
115. Bassler, R.S. Treatise on Invertebrate Paleontology. In *Part G, Bryozoa*; Moore, R.C., Ed.; Geological Society of America: Boulder, CO, USA; University of Kansas of Kansas Press: Lawrence, KS, USA, 1953; p. 253.

116. Stumm, E.C.; Wright, J.D. Check list of fossil invertebrates described from the Middle Devonian rocks of the Thedford-Arkona Region of southwestern Ontario. *Contrib. Mus. Paleontol. Univ. Mich.* **1958**, *14*, 81–132.
117. Olempska, E. Exceptional soft-tissue preservation in boring ctenostome bryozoans and associated “fungal” borings from the Early Devonian of Podolia, Ukraine. *Acta Palaeontol. Pol.* **2012**, *57*, 925–940. [[CrossRef](#)]
118. Wilson, M.A.; Taylor, P.D. The Paleozoic encrusting sclerobionts *Allonema* and *Ascodictyon*: Component parts of organisms belonging to the same problematic group. *Geol. Soc. Am. Abstr. Program Annu. Meet.* **2013**, *45*, 300–311.
119. Wilson, M.A.; Taylor, P.D. The morphology and affinities of *Allonema* and *Ascodictyon*, two abundant Palaeozoic encrusters commonly misattributed to the ctenostome bryozoans. *Studi Trentini Scienze Naturali* **2014**, *94*, 259–266.
120. Wilson, M.A.; Palmer, T.J. Patterns in the Ordovician bioerosion revolution. *Ichnos* **2006**, *13*, 109–112. [[CrossRef](#)]
121. Taylor, P.D. Preservation of soft-bodied and other organisms by bioimmuration—A review. *Palaeontology* **1990**, *33*, 1–17.
122. Todd, J.A.; Taylor, P.D.; Favorskaya, T.A. A bioimmured ctenostome bryozoan from the early Cretaceous of the Crimea and the new genus *Simplicidium*. *Geobios* **1997**, *30*, 205–213. [[CrossRef](#)]
123. Todd, J.A.; Hagdorn, N.H. First record of Muschelkalk Bryozoa: The earliest ctenostome body fossils. In *Muschelkalk. Schöntaler Symposium 1991*; Hagdorn, H., Seilacher, A., Eds.; Sonderbände der Gesellschaft für Naturkunde in Württemberg 2; Goldschneck: Stuttgart, Germany, 1993; pp. 285–286.
124. Peel, J.S.; Jeppson, L. The problematic fossil *Jinonicella* from the Lower Silurian of Gotland. *GFF* **2006**, *28*, 39–42. [[CrossRef](#)]
125. Pokorný, V. *Jinonicellina*, a new suborder of presumed Archaeogastropoda. *Bull. Czech Geol. Surv.* **1978**, *53*, 39–42.
126. Dzik, J. Larval development, musculature, and relationships of *Sinuitopsis* and related Baltic bellerophonts. *Norsk Geol. Tidsskrift* **1981**, *61*, 111–121.
127. Dzik, J. Machaeridians, chitons, and conchiferan molluscs of the Mójca Limestone. *Acta Palaeontol. Pol.* **1994**, *53*, 213–252.
128. Peel, J.S. Scaphopodization in Palaeozoic mollusks. *Palaeontology*. **2006**, *49*, 1357–1364. [[CrossRef](#)]
129. Fryda, J. Taxonomic position of suborder *Jinonicellina*. *Bull. Czech Geol. Surv.* **1999**, *74*, 27–29.
130. Yochelson, E.L. Comments on *Janospira*. *Lethaia* **1977**, *10*, 204. [[CrossRef](#)]
131. Love, L.G.; Zimmerman, D.O. Bedded pyrite and micro-organisms from the Mount Isa Shale. *Econ. Geol.* **1961**, *56*, 873–896. [[CrossRef](#)]
132. Love, L.G.; Murray, J.W. Biogenic pyrite in recent sediments of Christchurch Harbour, England. *Am. J. Sci.* **1983**, *261*, 433–448. [[CrossRef](#)]
133. Kohn, M.J.; Riciputi, L.R.; Stakes, D.; Orange, D.L. Sulfur isotope variability in biogenic pyrite: Reflections of heterogeneous bacterial colonization. *Am. Mineral.* **1998**, *83*, 1454–1468. [[CrossRef](#)]
134. Folk, R. Nannobacteria and the formation of framboidal pyrite: Textural evidence. *J. Earth Syst. Sci.* **2005**, *114*, 369–374. [[CrossRef](#)]
135. Maclean, L.C.W.; Tyliczszak, T.; Gilbert, P.U.P.A.; Zhou, D.; Pray, T.J.; Onstott, T.C.; Southam, G. A high-resolution chemical and structural study of framboidal pyrite within a low-temperature bacterial biofilm. *Geobiology* **2008**, *6*, 471–480. [[CrossRef](#)] [[PubMed](#)]
136. Love, L.G. Early diagenetic iron sulphide in recent sediments of the Wash (England). *Sedimentology* **1967**, *9*, 327–352. [[CrossRef](#)]
137. Lein, A.Y. Formation of carbonate and sulfide minerals during diagenesis of reduced sediment. In *Environmental Biogeochemistry and Geomicrobiology*; Krumbein, W.E., Ed.; Ann Arbor Science: Ann Arbor, MI, USA, 1978; pp. 339–354.
138. Allison, P.A. The role of anoxia in the decay and mineralization of proteinaceous macro-fossils. *Paleobiology* **1988**, *14*, 139–154. [[CrossRef](#)]
139. Rickard, D.T.; Schoonen, M.A.A.; Luther, G.W. Chemistry of iron sulfides in sedimentary environments. In *Geochemical Transformations of Sedimentary Sulfur*; American Chemical Society Symposium Series, v. 612; Vairavamurthy, M.A., Schoonen, M.A.A., Eds.; American Chemical Society: Washington, DC, USA, 1995; pp. 168–193.

140. Wilkin, R.T.; Barnes, H.L. Pyrite formation by reactions of iron monosulfides with dissolved inorganic and organic sulfur species. *Geochim. Cosmochim. Acta* **1996**, *60*, 4167–4179. [[CrossRef](#)]
141. Wilkin, R.T.; Barnes, H.L. Formation processes of framboidal pyrite. *Geochim. Cosmochim. Acta* **1997**, *61*, 323–339. [[CrossRef](#)]
142. Ettensohn, F.R. Controls on development of Catskill Delta complex basin-facies. In *The Catskill Delta*; Geological Society of America Special Paper 201; Woodrow, D.L., Sevon, W.D., Eds.; Geological Society of America: Boulder, CO, USA, 1985; pp. 65–77.
143. Stasiuk, L.D.; Fowler, M.G. Organic facies in Devonian and Mississippian strata of Western Canada Sedimentary Basin: Relation to kerogen type, paleoenvironment, and paleogeography. *Bull. Can. Petrol. Geol.* **2004**, *52*, 234–255.
144. Baird, G.C.; Brett, C.E. Late Middle Devonian (Late Givetian) Tully Formation in Pennsylvania: Comparison with Tully Limestone and equivalent clastic deposits in New York State. *Geol. Soc. Am. Abstr. Program Annu. Meet.* **2007**, *39*, 39.
145. Wignall, P.B.; Hallam, A. Biofacies, stratigraphic distribution and depositional models of British onshore Jurassic black shales. In *Modern and Ancient Continental Shelf Dysoxia*; Special Publication 58; Tyson, R.V., Pearson, T.H., Eds.; Geological Society London: London, UK, 1991; pp. 291–309.
146. Allison, P.A.; Wignall, P.B.; Brett, C.A. Palaeo-oxygenation: Effects and recognition. In *Marine Palaeoenvironmental Analysis from Fossils*; Special Publication 83; Bosence, D.W.J., Allison, P.A., Eds.; Geological Society London: London, UK, 1995; pp. 97–112.
147. Boyer, D.I.; Droser, M.I. Palaeoecological patterns within the dysaerobic biofacies: Examples from Devonian black shales of New York State. *Palaeogeogr. Palaeoclimatol. Palaeoecol.* **2009**, *276*, 206–216. [[CrossRef](#)]
148. Mapes, R.H.; Nützel, A. Late Palaeozoic mollusc reproduction: Cephalopod egg-laying behavior and gastropod larval palaeobiology. *Lethaia* **2009**, *42*, 341–356. [[CrossRef](#)]
149. Arnold, J.M.; Carlson, B.A. Living *Nautilus* embryos: Preliminary observations. *Science* **1986**, *232*, 73–76. [[CrossRef](#)] [[PubMed](#)]
150. Okubo, S.; Tsujii, T.; Watabe, N.; Williams, D.F. Hatching of *Nautilus belauensis* Saunders 1981, in captivity: Culture, growth and stable isotope compositions of shells, and histology and immunohistochemistry of the mantle epithelium of the juveniles. *Veliger* **1995**, *38*, 192–202.



© 2016 by the authors; licensee MDPI, Basel, Switzerland. This article is an open access article distributed under the terms and conditions of the Creative Commons Attribution (CC-BY) license (<http://creativecommons.org/licenses/by/4.0/>).